

Two-photon processes in e^+e^- calorimetric experiments and tests of quantum chromodynamics

M. Abud, R. Gatto, and C. A. Savoy

Département de Physique Théorique, Université de Genève, 1211 Genève 4, Switzerland

(Received 24 May 1979)

High-energy two-photon collisions will be responsible for a large fraction of events in e^+e^- machines such as PETRA, PEP, and LEP. We suggest measuring the energy pattern of the $\gamma\gamma$ processes, which would provide very interesting information on the interplay between electromagnetic and strong interactions. The angular distribution of the hadronic energy (antenna pattern) is calculated for photon-photon collisions. By using energy-conservation sum rules, we give a model-independent, reliable computation of the corrections due to color confinement, as well as heavy-quark masses and decays. The contributions from the quantum chromodynamics (QCD) structure of the photon, which are characterized by three or four jets in the final state, are taken into account. The energy correlation, i.e., the hadronic energy radiated through two calorimeters as a function of the relative angle is also calculated. We evaluate the energy pattern and energy correlation for the formation of C -even bound states, and find that an extremely good resolution in the hadronic energy would be needed in order to disentangle the bound-state contribution from the background. We present a detailed discussion of the two-photon processes as a background in the studies of the energy pattern of the e^+e^- annihilation into hadrons. By requiring that either the total hadronic energy or the invariant hadronic mass is larger than 60% of their maximum value, \sqrt{s} , the $\gamma\gamma$ background should be suppressed enough to allow for the experimental tests of QCD in e^+e^- annihilation which have been recently proposed.

I. INTRODUCTION

Strong interactions look much simpler at high energies, offering some support for quantum chromodynamics (QCD) as the underlying theory. The essential point in our present understanding of short-distance phenomena has been asymptotic freedom which characterizes non-Abelian gauge theories such as QCD. It allows for a rather special use of perturbative calculations in terms of the running coupling constant $\alpha_s(s)$ which becomes small at high energies. Actually, the present-day approach to short-distance processes consists of two steps: a quark (and gluon) interaction involving large momentum transfers, followed by the color recombination, when confined quarks materialize into the final hadrons in a rather soft way, in the sense that energy transfers are now small. The hard interaction between quarks is assumed to be described by perturbative QCD. However, only those experimental quantities are computable which are free from mass singularities. This in turn requires the use of inclusive observables, whose prototype is the total cross section for electron-positron annihilation into hadrons.

Recently, Basham *et al.*¹ suggested that a whole class of angular distributions should be free of mass singularities and then calculable in perturbative QCD. Further support to their arguments has been presented by Tiktopoulos.² The simplest experimental quantity studied by these authors is the energy angular distribution in e^+e^- collisions,

the so-called "antenna pattern."³ It is defined to be the hadronic energy radiated through a unit solid angle in a given direction, divided by the incident energy per unit area.

This antenna pattern is also very suitable from the experimentalist point of view. At high energies most of the events consist of many particles, in several flavors, so that the identification of each particle becomes a hard task, requiring ingenious apparatuses and reducing the acceptances. Moreover, it actually gives only secondary information on the nature of strong interactions which are much more concerned with colors than flavors (with the important exception of the electric charge, since the strong interacting fermions are charged while gluons are neutral). This fact sharply supports the use of calorimeters, to measure the angular distribution of the hadronic energy flow resulting from the interaction, as the primordial experimental arrangement in the study of high-energy reactions. It is a remarkable, but not coincidental fact, that these calorimetric measures are related to a calculable quantity.¹ The color confinement will affect the antenna pattern in the sense of a spread of the quark (gluon) energy due to the hadronization process. Since this is a non-perturbative phenomenon, its description has to be done in terms of the empirical fragmentation functions.³ A welcome feature of the antenna pattern is that the nonperturbative corrections from the quark confinement can be reliably estimated from these two general characteristics, independently of the detailed form of the fragmentation functions.

The net effect of the confinement corrections is a broadening of the angular distribution that is proportional to the opening angle of the hadronic jet, which is as small as $\langle p_T \rangle / \sqrt{s}$ at higher energies, $\langle p_T \rangle$ being the mean transverse momentum of hadrons in the jet.¹

Another quantity which has the same characteristics is the so-called energy correlation. In this case, one measures the energy radiated through *two* calorimeters as a function of the angle between them. The fragmentation of the quark and its antiquark, which come out back-to-back in their c.m. system, give an energy correlation symmetric under the exchange of the resulting jets to order $\langle p_T \rangle / \sqrt{s}$, which is the magnitude of the jet opening angle. Instead, the QCD corrections to order $\alpha_s(s)$ introduce an asymmetry in the energy correlation from the fact that a gluon is emitted from either one or the other quark. This provides for an elegant test of QCD in e^+e^- collisions.¹

In the calculation of angular distributions one must take care of the threshold effects in the production of heavy quarks. They are of three kinds: (i) bound states and resonances, (ii) dependence of the production cross sections on m_Q/\sqrt{s} and (iii) the weak decay of heavy hadrons holding the heavy quark after the fragmentation. The resonances and bound states can be avoided by working a few GeV aside their region. The corrections from the heavy-quark mass and decay could be more difficult to eliminate, since they are more persistent. The obvious way to reduce their effect is to go to an energy region which is far enough from $Q\bar{Q}$ thresholds. However, there is no pungent reason to believe that such an energy region exists inside the range of present accelerators (PETRA, PEP) or even of the next-generation ones (LEP). One can easily imagine a situation where a new quark threshold opens before the mass and decay effects of the preceding quarks become small. Interestingly enough, the antenna pattern for heavy quarks can be precisely computed in a way which is essentially model-independent, a trivial energy-conservation sum rule eliminating the dependence on the branching ratios, spectra, and multiplicities of the weak decays.

It is very well known that QED corrections to e^+e^- collisions become important at high energies.⁴ In the hadronic channel, the relevant processes are $\gamma\gamma$ collisions, $e^+e^- \rightarrow (e^+e^-)\gamma\gamma \rightarrow (e^+e^-)$ hadrons.^{4,5} The essential contribution, which is proportional to $\alpha \ln(\sqrt{s}/m_Q)$, corresponds to the final leptons going almost along the beams, with the interacting photons virtually on-shell.⁶ In most of the experiments the final e^+e^- pair is not tagged, but the $\gamma\gamma$ processes differ from the e^+e^- annihilation by the fact that the total hadronic energy and

the invariant hadronic mass of the final states are less than \sqrt{s} for the former. Indeed, the largest part of the 2γ -originated hadronic final state will present low multiplicity and come out at small angles (small transverse momentum). By measuring at least one of these quantities, one can choose suitable cuts, in order to select events which are mostly from one-photon processes, and so the two-photon contribution can be reduced to a tolerable amount.⁷ This procedure is slightly easier in the measure of the antenna pattern and energy correlation since the events are, by definition, weighted by their hadronic energies.

In this paper, we make a careful study of the contribution to the energy correlation and antenna pattern from $\gamma\gamma$ collisions. We then discuss how to disentangle the one-photon and the two-photon components in calorimeter experiments. Since the ultimate purpose of these measurements could be to test QCD as suggested in Ref. 1, the suppression of the two-photon-originated events should be very efficient. We shall conclude that QCD could be tested in principle if one is able to select those events with either total hadronic energy or invariant hadronic mass larger than about 60%–70% of their maximum value, \sqrt{s} . The first alternative looks particularly interesting since it could be more easily achieved in calorimeter experiments.

As a matter of fact, $\gamma\gamma$ physics is a very important field in its own, which would contribute to a great extent to our knowledge of both the electromagnetic and the strong interactions of hadrons.^{4,5,8-10} In the light of our present belief in QCD as the theory of hadronic matter, this is particularly true for $\gamma\gamma$ collisions at high energies, large momentum transfers, such that asymptotic freedom and perturbation theory can be applied. But, as already stressed, one has to look carefully for those observables which are free from mass singularities.

In this paper, we suggest measuring the antenna pattern and the energy correlation as a function of the hadronic invariant mass (or, possibly, the total hadronic energy) in $\gamma\gamma$ collisions. This would provide very interesting information on the quark interactions, as well as a determination of $(\sum_i Q_i^4)$ as a function of the available energy for quark production.

Perhaps the most exciting experiment in $\gamma\gamma$ physics is the test of the QCD structure of the photon. As first pointed out by Witten,⁹ the structure functions of the photon are completely computable at very large momentum transfer in QCD. They can be presumably measured in photon-photon scattering. This possibility will be discussed in Secs. VII and VIII, from the viewpoint of calorimeter experiments.

Another interesting aspect of two-photon physics is the formation of quark-antiquark bound states with even C parity. The contributions of these bound states to the antenna pattern can be evaluated through the use of semiclassical sum rules. These angular distributions are very different from the background, which is essentially due to the production of light quarks. Unfortunately, our calculations indicate that the separation of the bound-state contribution should be presumably unfeasible.

The paper is organized as follows. The formalism is developed in Secs. II, III, V–VII, while most of the numerical results are presented and discussed in Secs. IV and VIII, with particular emphasis on the energies in the ranges of PETRA/PEP and LEP performances. Expressions for the antenna pattern and energy correlation in two-photon processes are calculated: in Secs. II and III for the production of light quarks, in Sec. V for the formation of $Q\bar{Q}$ bound states, in Sec. VI for the production of (weakly decaying) heavy quarks. Section VII contains a brief discussion of the importance of the photon structure functions, as well as the calculation of their contribution to the antenna pattern. Confinement corrections and effects from quark masses and decays are studied in detail and presented in four Appendices. In Sec. IV the one-photon and the two-photon contributions to the antenna pattern and energy correlation are compared and possible ways to disentangle them are discussed. In Sec. VIII we present our numerical estimates of the antenna pattern at fixed values of the total hadronic invariant mass. We end with a few remarks in Sec. IX.

II. ANTENNA PATTERN FOR $e^+e^- \rightarrow e^+e^-\bar{q}q$

We will perform our calculations in the equivalent-photon approximation (EPA). In most of the experiments the scattered electrons are not tagged and the dominant contributions to the cross sections are from processes where the radiated photons acquire a negligible transverse momentum and are almost onshell. In EPA, one then assumes that the processes of the type $e^+e^- \rightarrow e^+e^-\gamma\gamma$

$\rightarrow e^+e^- + \text{hadrons}$ are well described by the process $\gamma\gamma \rightarrow \text{hadrons}$ with an equivalent flux obtained by taking the limit of the Feynman diagrams where the photons are on-shell. One obtains for the cross sections in EPA

$$d\sigma(s)_{(e^+e^- \rightarrow e^+e^- + \text{hadrons})} = \int_0^1 \frac{dx_1}{x_1} \int_0^1 \frac{dx_2}{x_2} N(x_1)N(x_2) \times d\sigma_{(\gamma\gamma \rightarrow \text{hadrons})}(x_1, x_2, s), \quad (2.1)$$

where \sqrt{s} is the total energy, $x_1\sqrt{s}/2$ and $x_2\sqrt{s}/2$ are the fractions of the e^+ and e^- energies carried by the radiated photons in the e^+e^- c.m. system, and $x_1x_2s = M_H^2$ is the square of the invariant mass of the produced hadronic system. In the leading-logarithm approximation, which is valid for $\ln(\sqrt{s}/m_e) \gg 1$, $N(x)$ is given by

$$N(x) = \frac{\alpha}{\pi} \ln\left(\frac{\sqrt{s}}{2m_e}\right) [1 + (1-x)^2]. \quad (2.2)$$

It can be interpreted in Eq. (2.1) as being the momentum distribution of the radiated interacting photon. It is convenient to work with all energies and momenta given in units of \sqrt{s} . We introduce the following notation:

$$\tau = x_1x_2, \quad \zeta = \frac{x_1+x_2}{2}, \quad \xi = \frac{x_1-x_2}{2}, \quad (2.3)$$

$$v = \frac{\xi}{\zeta} = \frac{x_1-x_2}{x_1+x_2}, \quad \tau = \zeta^2 - \xi^2,$$

where $\sqrt{\tau s} = M_H$ is the invariant mass of the two-photon system, $\zeta\sqrt{s}$ and $\xi\sqrt{s}$ are the total energy and momentum of the two interacting photons, and v is the velocity of the 2γ c.m. frame in the colliding-beam c.m. system. For any produced particle, the scattering angles, θ in the e^+e^- c.m. system, and θ^* in the 2γ c.m. system, are related by the appropriate Lorentz boost as follows:

$$\cos\theta^* = \frac{\cos\theta - v}{1 - v\cos\theta}, \quad \cos\theta = \frac{\cos\theta^* + v}{1 + v\cos\theta^*}. \quad (2.4)$$

In EPA, the hadron inclusive differential cross section in the e^+e^- c.m. and the antenna pattern are given by

$$\frac{d\sigma}{d\Omega} = \int_0^1 \frac{dx_1}{x_1} N(x_1) \int_0^1 \frac{dx_2}{x_2} N(x_2) \sum_i \int \frac{d^3\vec{p}_i}{2E_i} \frac{d\hat{\sigma}_i(x_1, x_2, s)}{(d^3\vec{p}_i/2E_i)} \delta(\Omega - \Omega_i), \quad (2.5)$$

$$\frac{d\Sigma}{d\Omega} = \int_0^1 \frac{dx_1}{x_1} N(x_1) \int_0^1 \frac{dx_2}{x_2} N(x_2) \sum_i \int \frac{d^3\vec{p}_i}{2E_i} \frac{d\hat{\sigma}_i(x_1, x_2, s)}{(d^3\vec{p}_i/2E_i)} \frac{E_i}{\sqrt{s}} \delta(\Omega - \Omega_i),$$

where the index i runs over the produced particles and $\hat{\sigma}_i$ is the $\gamma\gamma \rightarrow i$ inclusive cross section. The

noncovariant components of Eq. (2.5) (E_i and Ω_i, Ω) can be transformed by a Lorentz boost and we get,

by introducing the variables (2.3),

$$\frac{d\sigma}{d\Omega} = \int \frac{d\tau}{\tau} \int \frac{d\xi}{\xi} \frac{N(\xi + \tau)N(\xi - \tau)}{(\xi - \tau \cos\theta)^2} \tau \frac{d\hat{\sigma}(\tau s)}{d\Omega^*}, \quad (2.6)$$

$$\frac{d\Sigma}{d\Omega} = \int \frac{d\tau}{\tau} \int \frac{d\xi}{\xi} \frac{N(\xi + \tau)N(\xi - \tau)}{(\xi - \tau \cos\theta)^3} \tau^2 \frac{d\hat{\sigma}(\tau s)}{d\Omega^*}.$$

Here $d\sigma/d\Omega^*$ and $d\Sigma^*/d\Omega^*$ are the inclusive cross section and the antenna pattern for the $\gamma\gamma \rightarrow$ hadrons process in the 2γ c.m. system; the angle θ^* is related to θ by Eq. (2.4).

One can now distinguish between two possible experimental situations:

- (a) The invariant mass $\sqrt{\tau s}$ of the whole system of produced hadrons is measured to some extent.
- (b) Only the total energy of the final hadrons can be measured.

In (a) one can select those events whose total invariant mass $\sqrt{\tau}$ (in units of \sqrt{s}) is larger than some minimum value $\sqrt{\tau_0}$. In this way one could eliminate the events with small values of $\sqrt{\tau}$, which give most of the contributions to the $e^+e^- \rightarrow e^+e^- +$ hadrons cross section. However, in order to do so (in a calorimeter-type experiment), in principle, one has to measure the energy through each element $\Delta\Omega$ of solid angle in *all* directions for each event.

In (b) one can use a simpler experimental setup, but in order to depress the contribution from 2γ processes one has to require that the total energy ξ (in units of \sqrt{s}) of the accepted events in the e^+e^- c.m. system be larger than some fraction ξ_0 of the colliding beams energy \sqrt{s} . In some sense, case (b) is more in the spirit of a calorimeter experiment. However, as already stressed in the introduction, this procedure could be inefficient since, at fixed energy ξ , the events tend to be concentrated in the region where the invariant mass $\sqrt{\tau}$ is small. This corresponds to events with only a few particles being produced within a small solid angle around one of the beams. The production of such hadronic system with low invariant mass is typically a problem of confined quarks and, therefore, it could be hardly estimated. The best thing to do is to prevent the data from the potentially huge contamination by these events, by an experimental cut $\sqrt{\tau_0}$ on the mass of the hadronic system $\sqrt{\tau}$. Interestingly enough one can do that without going back to case (a), by a convenient choice of the lower cut ξ_0 on the total energy. This possibility, which results in a simple but efficient experimental tool, follows from a trivial kinematical condition. Since both x_1 and x_2 in Eqs. (2.3) take values between 0 and 1, one has the condition

$$\tau = x_1 x_2 \geq 2\xi - 1 = x_1 + x_2 - 1. \quad (2.7)$$

For $\xi \leq \frac{1}{2}$ this condition is trivially satisfied.

But for $\xi = \frac{1}{2} + \epsilon > \frac{1}{2}$ one gets $\tau > 2\epsilon$. Therefore, by choosing

$$\xi_0 = \frac{1 + \tau_0}{2} \quad (\tau_0 > 0) \quad (2.8)$$

as the experimental cut on the total hadronic energy in the calorimeter, one can eliminate all the events with $M_H^2 < \tau_0 s$.

It is convenient to write the antenna pattern, Eq. (2.6), in one of the following forms:

$$\frac{d\Sigma}{d\Omega} = \int_{\tau_0}^1 \frac{d\tau}{\tau^{3/2}} \int_{(\tau-1)/(\tau+1)}^{(1-\tau)/(1+\tau)} dv (1-v^2)^{1/2} \frac{N(\tau, v)N(\tau, -v)}{(1-v \cos\theta)^3} \times \tau \left(\frac{d\Sigma^*}{d\Omega^*} \right), \quad (2.9a)$$

$$\frac{d\Sigma}{d\Omega} = 2 \int_{\xi_0}^1 \frac{d\xi}{\xi^2} \int_{-v_0(\xi)}^{v_0(\xi)} dv \frac{N(\xi, v)N(\xi, -v)}{(1-v \cos\theta)^3} \tau \left(\frac{d\Sigma^*}{d\Omega^*} \right), \quad (2.9b)$$

where [cf. Eq. (2.2)]

$$v_0 = \text{Min} \left[\frac{1-\xi}{\xi}, \left(1 - \frac{\tau_0}{\xi^2} \right)^{1/2} \right],$$

$$N(\tau, v)N(\tau, -v) = C(s) \left[1 + \frac{\tau^2}{4} + \frac{2\tau}{1-v^2} - \frac{\sqrt{\tau}(2+\tau)}{(1-v^2)^{1/2}} \right]$$

$$= N(\xi, v)N(\xi, -v)$$

$$= C(s) \left[1 - 2\xi + 2\xi^2 - \xi^3(1-v^2) + \frac{1}{4}\xi^4(1-v^2)^2 \right], \quad (2.10)$$

$$C(s) = \left(\frac{\alpha}{\pi} \ln \frac{s}{4m_e^2} \right)^2.$$

Equation (2.9a) applies to case (a) for an experimental cut $\tau > \tau_0$ on the data, while Eq. (2.9b) is to be used in case (b) for a cut $\xi > \xi_0$ on the total calorimeter energy.

In order to evaluate Eqs. (2.9a) and (2.9b) the antenna pattern for the process $\gamma\gamma \rightarrow$ hadrons is needed. If the invariant mass of the 2γ system is large, this process can be estimated in a simple perturbative approach. Assuming asymptotic freedom, one has to calculate $\gamma\gamma \rightarrow \bar{q}q$ to lowest order. If needed, one can take into account radiative corrections to the appropriate order in α_s . As remarked in the Introduction, this calculation make sense, provided $\alpha_s \ll 1$, because the antenna pattern should not have mass singularities in the perturbative expansion. For the purposes of this paper it is enough to use the lowest-order expression for the antenna pattern of the process $\gamma\gamma \rightarrow \bar{q}q$, which reads

$$\begin{aligned} \frac{d\Sigma^*}{d\Omega^*} &= \frac{d\sigma^*}{d\Omega^*} \\ &= \frac{\alpha^2 Q^4}{\tau s} \left[\beta + 2\beta^3 \frac{1 - \beta^2 + \beta^2 \cos^2 \theta^* - \beta^2 \cos^4 \theta^*}{(1 - \beta^2 \cos^2 \theta^*)^2} \right], \end{aligned} \quad (2.11)$$

where Q is the charge of the quark in units of e , and β is its velocity in the 2γ c.m. system,

$$\beta = \left(1 - \frac{4m_q^2}{s} \right)^{1/2}. \quad (2.12)$$

By adding the contribution of all light quarks, one gets in the limit $m_q^2/s \rightarrow 0$, $\beta \rightarrow 1$,

$$\begin{aligned} \tau \frac{d\Sigma^*}{d\Omega^*} &= \frac{\alpha^2}{s} \left(3 \sum_f Q_f^4 \right) \left(\frac{2}{\sin^2 \theta^*} - 1 \right) \\ &= \frac{\alpha^2}{s} \left(3 \sum_f Q_f^4 \right) \left(\frac{2(1 - v \cos \theta)^2}{(1 - v^2) \sin^2 \theta} - 1 \right). \end{aligned} \quad (2.13)$$

This calculations can be improved by the addition of the so-called confinement corrections. This is done on phenomenological grounds by implementing Eq. (2.13) with the fragmentation functions of quarks into hadrons. As already noticed by Basham *et al.* in the simpler case of the 1γ contribution, the confinement corrections to the antenna pattern are proportional to $\langle p_T \rangle / \sqrt{s}$, where $\langle p_T \rangle$ is the average transverse momentum of hadrons in a quark jet (empirically, $\langle p_T \rangle \sim 300$ MeV). This is shown in Appendix A, where the confinement corrections are calculated and discussed in detail.

As a matter of fact, one expects the jet spreading from QCD radiative corrections to be more important than the confinement effects at very high energies. Contributions from the QCD structure of the photon, which are discussed in Sec. VII, should also have a significant magnitude. However, the main aim of Sec. IV being to compare the 2γ contributions with the QCD radiative corrections to the one-photon antenna pattern; the QCD corrections to the 2γ processes should not have any relevance in our discussions there.

Let us first consider the simpler case (b) above and assume that the experimental cut on the total energy is in the interesting region $\xi_0 = \frac{1}{2}(1 + \tau_0) > \frac{1}{2}$. Inserting Eq. (2.13) into Eq. (2.9b) one gets

$$\begin{aligned} \frac{d\Sigma}{d\Omega} &= \frac{\alpha^2}{s} \left(12 \sum_f Q_f^4 \right) C(s) \\ &\times \int_{\xi_0}^1 \frac{d\xi}{\xi^2} \int_0^{(1-\xi)/\xi} dv H(\xi, v) F(v, \theta), \end{aligned} \quad (2.14)$$

with

$$\begin{aligned} F(v, \theta) &= \frac{2}{(1 - v^2) \sin^2 \theta (1 - v^2 \cos^2 \theta)} \\ &- \frac{1 + 3v^2 \cos^2 \theta}{(1 - v^2 \cos^2 \theta)^3}, \end{aligned} \quad (2.15)$$

$$H(\xi, v) = 1 - 2\xi + 2\xi^2 - \xi^3(1 - v^2) + \xi^4(1 - v^2)^2/4.$$

This can also be written in the following way:

$$\begin{aligned} \frac{d\Sigma}{d\Omega} &= \frac{\alpha^2}{s} A_{\gamma\gamma}(\theta, \xi_0), \\ A_{\gamma\gamma}(\theta, \xi_0) &= 12 \left(\sum_f Q_f^4 \right) C(s) \\ &\times \int_0^{(1-\xi_0)/\xi_0} dv F(v, \theta) \mathcal{J}(\xi_0, v), \end{aligned} \quad (2.16)$$

$$\begin{aligned} \mathcal{J}(\xi_0, v) &= \frac{1}{\xi_0} - 2\xi_0 + \frac{\xi_0^2(1 - v^2)}{2} - \frac{\xi_0^3(1 - v^2)^2}{12} \\ &+ 2 \ln[\xi_0(1 + v)] - \frac{11}{12}(1 + v) + \frac{1}{6} + \frac{4}{3(1 + v)}. \end{aligned}$$

This antenna pattern is shown, in units of α^2/s , in Fig. 1, for $\sqrt{s} = 30$ GeV. The very simple ex-

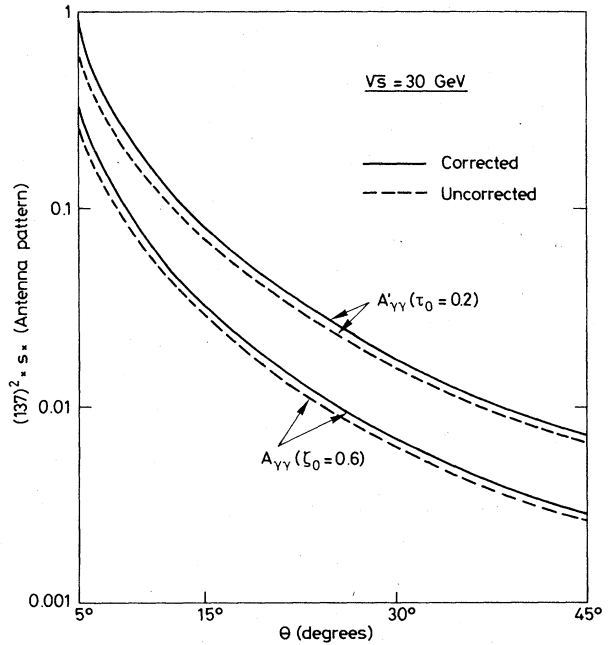


FIG. 1. Angular distribution of the energy flow (antenna pattern) for $\gamma\gamma$ collisions in units of α^2/s . The dashed lines are the antenna pattern at small distances and the solid lines are the corresponding results after the color confinement corrections are included. As explained in the text, in $A_{\gamma\gamma}(\xi_0)$ only events with hadronic energy $E_H > \xi_0 s^{1/2}$ are taken into account, while $A'_{\gamma\gamma}(\tau_0)$ is the antenna pattern of events with total hadronic invariant mass $M_H > (\tau_0 s)^{1/2}$.

pression

$$A_{\gamma\gamma}(\theta, \xi_0) \approx (2.85 \times 10^{-5}) \left(3 \sum_f Q_f^4 \right) \times \left(\ln \frac{s}{4m_e^2} \right) (2\xi_0)^{-15/2} \left(\frac{1 + \cos^2\theta}{1 - \cos^2\theta} \right) \quad (2.17)$$

fits Eq. (2.16) with an accuracy which is better than 20% for $\xi > 0.52$, $\theta > 5^\circ$. It is worth noticing that (i) there is a strong dependence on the ξ_0 cut, (ii) the antenna for $e^+e^- \rightarrow e^+e^- +$ hadrons has roughly the same angular distribution as the antenna for the elementary ($\gamma\gamma \rightarrow$ hadrons) process.

This expression has to be corrected for the quark confinement by the addition of the term $A_{\gamma\gamma}^{cc}$, defined in Appendix A. A discussion of the numerical results is presented in Sec. IV.

As already remarked, these expressions are only valid in the asymptotically free region, which here is defined by $\alpha_s(\tau_0 s) \ll 1$, corresponding to values of $(\tau_0 s)^{1/2} = [(2\xi_0 - 1)s]^{1/2}$ larger than a few GeV.

Let us now consider the more sophisticated experiments of the kind (a) above, where one assumes that those events with $M_H^2 < \tau_0 s$ have been eliminated from the data. The value of τ_0 has to be chosen such that $(\tau_0 s)^{1/2}$ is large enough (more than a few GeV) in order to exclude the "resonance region" where our approximations do not apply. From Eqs. (2.9a) and (2.13) one then gets

$$\begin{aligned} \frac{d\Sigma}{d\Omega} &= \frac{\alpha^2}{s} A'_{\gamma\gamma}(\tau_0, \theta), \\ A'_{\gamma\gamma}(\tau_0, \theta) &= 6 \left(\sum_f Q_f^4 \right) C(s) \\ &\times \int_{\tau_0}^1 \frac{d\tau}{\tau^{3/2}} \int_0^{(1-\tau)/(1+\tau)} dv \tilde{H}(\tau, v) F(v, \theta), \\ \tilde{H}(\tau, v) &= (1 + \frac{1}{4}\tau^2)(1 - v^2)^{1/2} \\ &+ \frac{2\tau}{(1 - v^2)^{1/2}} - \sqrt{\tau}(2 + \tau), \end{aligned} \quad (2.18)$$

and $F(v, \theta)$ is the function defined in Eq. (2.15).

This antenna pattern is shown in Fig. 1 for $\sqrt{s} = 30$ GeV. For τ_0 not too small, $\tau_0 > 0.01$, one can evaluate $A'_{\gamma\gamma}$ from the simple fit:

$$A'_{\gamma\gamma}(\tau_0, \theta) \approx (1.0 \times 10^{-6}) \left(3 \sum_f Q_f^4 \right) \left(\ln \frac{s}{4m_e^2} \right)^2 \times \frac{(1 - \tau_0)^{9/4}}{\tau_0^{5/4}} \left(\frac{1 + \cos^2\theta}{1 - \cos^2\theta} \right), \quad (2.19)$$

which reproduces Eq. (2.18) with a (10%–20%) accuracy. Again, the angular dependence of the $\gamma\gamma$ processes is not much affected by the weighted average on the velocity v .

A useful quantity in order to study $\gamma\gamma$ processes would be the differential antenna pattern as a function of the hadronic invariant mass $\sqrt{\tau}$ (in units of \sqrt{s}):

$$\begin{aligned} \frac{d\Sigma}{d\sqrt{\tau}d\Omega} &= \frac{\alpha^2}{s} a(\tau_0, \theta), \\ a(\tau_0, \theta) &= 12 \left(\sum_f Q_f^4 \right) \frac{C(s)}{\tau} \\ &\times \int_0^{(1-\tau)/(1+\tau)} dv \tilde{H}(\tau, v) F(v, \theta). \end{aligned} \quad (2.20)$$

This antenna pattern at fixed hadronic mass will be discussed in Sec. VIII.

III. ENERGY CORRELATION FOR $e^+e^- \rightarrow e^+e^-q\bar{q}$

We will discuss here the contribution of the two-photon processes to the energy correlation. As in Sec. II, the calculations will be performed in the equivalent-photon approximation (EPA). The notations are the same as in Sec. II.

From Eqs. (2.1) and (2.5) one obtains for the 2γ contribution to the energy correlation

$$\frac{d^2\Sigma}{d\Omega d\Omega'} = \int_0^1 \frac{dx_1}{x_1} \int_0^1 \frac{dx_2}{x_2} N(x_1)N(x_2) \sum_{i,j} \int d^3\vec{p}_i \int d^3\vec{p}_j \frac{d\hat{\sigma}_{ij}(x_1, x_2, s)}{d^3\vec{p}_i d^3\vec{p}_j} \frac{E_i E_j}{s} \delta(\Omega - \Omega_i) \delta(\Omega' - \Omega_j), \quad (3.1)$$

where $\hat{\sigma}_{ij}$ is the $\gamma\gamma \rightarrow i+j$ inclusive cross section, the indices i and j running over all the produced particles (the "transparent" term $i=j$ has also to be taken into account). With a Lorentz transformation of the non-covariant variables, Eq. (2.19) can be written in the form

$$\frac{d^2\Sigma}{d\Omega d\Omega'} = \int \frac{d\tau}{\tau} \int \frac{d\xi}{\xi} \frac{N(\xi + \xi)N(\xi - \xi)}{(\xi - \xi \cos\theta)^3 (\xi - \xi \cos\theta')^3} \tau^4 \frac{d^2\Sigma^*}{d\Omega^* d\Omega'^*}, \quad (3.2)$$

where $d^2\Sigma^*/d\Omega^*d\Omega'^*$ is the energy correlation for the $\gamma\gamma$ –hadrons process in the 2γ c.m. system; the angles θ^* and θ'^* in the 2γ c.m. system are related to θ and θ' through Eq. (2.4).

We can now use as integration variables the energy ξ and the velocity v , defined in Eq. (2.3), and we write

Eq. (3.2) as follows:

$$\frac{d^2\Sigma}{d\Omega d\Omega'} = 2 \int_{\tau_0}^1 \frac{d\xi}{\xi} \int_{-(1-\xi)/\xi}^{(1-\xi)/\xi} dv \frac{(1-v^2)^2 N(\xi, v) N(\xi, -v)}{(1-v \cos\theta)^3 (1-v \cos\theta')^3} \left(\frac{\tau d^2\Sigma^*}{d\Omega^* d\Omega'^*} \right). \quad (3.3)$$

We are interested here in the situation where the events with hadronic invariant mass M_H^2 less than some value $\tau_0 s$ are removed from the data. If $\tau_0 s$ is large enough (more than a few GeV, say), then the energy correlation for $2\gamma \rightarrow$ hadrons can be calculated through the $\gamma\gamma \rightarrow q\bar{q}$ subprocess (assuming asymptotic freedom). The confinement of quarks could be taken into account phenomenologically by using the fragmentation functions of quarks into hadrons. The QCD radiative corrections are more persistent, especially those related to the QCD structure functions of the photon. Since our aim in Sec. IV is to compare the order of magnitudes of the energy correlations in two-photon and one-photon processes, we will neglect these corrections until Sec. VII.

Within these approximations we identify the energy correlation for $\gamma\gamma \rightarrow$ hadrons to the $\gamma\gamma \rightarrow q\bar{q}$ one. For light quarks $m_q^2 \ll s$, the $\gamma\gamma \rightarrow q\bar{q}$ energy correlation is

$$\frac{\tau d^2\Sigma^*}{d\Omega^* d\Omega'^*} = \frac{\alpha^2}{2s} \left(3 \sum_f Q_f^4 \right) \frac{1 + \cos^2\theta^*}{1 - \cos^2\theta^*} \delta(\phi + \pi - \phi') \delta(\cos\theta^* + \cos\theta'^*), \quad (3.4)$$

where the δ functions correspond to the quarks going back to back in the two-body final state. By transforming θ^* and θ'^* into the e^+e^- c.m. angles θ and θ' , one gets

$$\frac{\tau d^2\Sigma}{d\Omega^* d\Omega'^*} = \frac{\alpha^2}{2s} \left(3 \sum_f Q_f^4 \right) \frac{\sin^2\left(\frac{\theta+\theta'}{2}\right) + \sin^2\left(\frac{\theta-\theta'}{2}\right)}{\sin^2\left(\frac{\theta+\theta'}{2}\right) - \sin^2\left(\frac{\theta-\theta'}{2}\right)} \frac{\sin^2\left(\frac{\theta+\theta'}{2}\right)}{2 \cos^2\left(\frac{\theta-\theta'}{2}\right)} \delta(\phi + \pi - \phi') \delta\left(v - \frac{\cos\left(\frac{\theta+\theta'}{2}\right)}{\cos\left(\frac{\theta-\theta'}{2}\right)}\right). \quad (3.5)$$

The δ function here relates the velocity v of the 2γ c.m. system to the scattering angles θ and θ' in the usual way.

The δ function on the azimuthal angles expresses the coplanarity of the final state, which is a trivial consequence of our approximations. It will be smeared out by the following effects:

(i) The angular spread of the photons relative to the initial electrons, which is not taken into account in the simple version of EPA considered here, is of the order of m_e/\sqrt{s} and can be safely neglected at high energies.

(ii) The opening of the jets from the confinement is expected to be of the order of $\langle p_T \rangle/\sqrt{s}$.

(iii) The QCD radiative corrections, which are proportional to α_s and then should decrease only as $(\ln s)^{-1}$. It should be dominant at very high energies.

The acoplanarity resulting from all these effects are expected to be small. We get rid of it by averaging on the azimuthal angles. We then insert Eq. (3.5) into Eq. (3.3), perform the trivial integrations on v and ϕ , and get for the energy correlation from the 2γ processes (averaged over the azimuthal angles)

$$\frac{d^2\Sigma}{d\Omega d\cos\theta'} = \frac{\alpha^2}{s} \left(3 \sum_f Q_f^4 \right) \frac{C(s)}{2} K(\theta, \theta') \times \int_{\tau_0}^1 \frac{d\xi}{\xi} H(\xi, \hat{v}) \theta(a(\xi) - \hat{v}), \quad (3.6)$$

$$\hat{v} = \left| \frac{\cos\left(\frac{\theta+\theta'}{2}\right)}{\cos\left(\frac{\theta-\theta'}{2}\right)} \right|,$$

where

$$K(\theta, \theta') = \frac{1}{\sin^4\left(\frac{\theta+\theta'}{2}\right)} \frac{\sin^2\left(\frac{\theta+\theta'}{2}\right) + \sin^2\left(\frac{\theta-\theta'}{2}\right)}{\left[\sin^2\left(\frac{\theta+\theta'}{2}\right) - \sin^2\left(\frac{\theta-\theta'}{2}\right) \right]^2},$$

$$H(\xi, \hat{v}) = 1 - 2\xi + 2\xi^2 - \xi^3(1 - \hat{v}^2) + \frac{1}{4}\xi^4(1 - \hat{v}^2)^2, \quad (3.7)$$

$$a(\xi) = \text{Min}\left(\left(1 - \frac{\tau_0}{\xi^2}\right)^{1/2}, (1 - \xi)/\xi \right).$$

The constant τ_0 is the experimental cut on the invariant mass of the final hadronic system. Now we can distinguish again the two experimental situations, (a) and (b), discussed in the Sec. II.

In case (b), the total energy of the produced hadrons in the e^+e^- c.m. system is required to be larger than some value $\xi_0\sqrt{s}$. As pointed out in Sec. II, in order to remove the huge contribution from events with low M_H , one has to take $\xi_0 \equiv \frac{1}{2}(1+\tau_0) > \frac{1}{2}$. Performing the ξ integration in Eq. (3.6) we obtain

$$\frac{d^2\Sigma}{d\Omega d\cos\theta'} = \frac{\alpha^2}{s} R_{\gamma\gamma}(\theta, \theta', \xi_0),$$

$$R_{\gamma\gamma}(\theta, \theta', \xi_0) = \left(3 \sum_f Q_f^4\right) \frac{C(s)}{2} K(\theta, \theta') I(\hat{v}, \xi_0), \quad (3.8)$$

$$I(\hat{v}, \xi_0) = \left\{ \frac{3\hat{v}^2 - 86\hat{v} - 61}{48(1+\hat{v})^2} - \ln[\xi_0(1+\hat{v})] \right. \\ \left. + 2\xi_0 - \xi_0^2 + \frac{\xi_0^3(1-\hat{v}^2)}{3} - \frac{\xi_0^4(1-\hat{v}^2)^2}{16} \right\} \theta(1-\xi_0(1+\hat{v})),$$

where $\tau_0 \equiv 2\xi_0 - 1 > 0$. The θ function defines the physical region.

In case (a), where the hadronic invariant mass is required to be larger than some value $\sqrt{\tau_0}\sqrt{s}$, Eq. (3.6) becomes

$$\frac{d^2\Sigma}{d\Omega d\cos\theta'} = \frac{\alpha^2}{s} \left(3 \sum_f Q_f^4\right) \frac{C(s)}{4} K(\theta, \theta') \\ \times \int_{\tau_0}^1 \frac{d\tau}{\tau} H\left(\left(\frac{\tau}{1-\hat{v}^2}\right)^{1/2}, \hat{v}\right) \theta\left(\frac{1-\tau}{1+\tau} - \hat{v}\right), \quad (3.9)$$

where the functions H and K , and the constant \hat{v} have been already defined in Eqs. (3.7) and (3.6), respectively. The integration over τ gives

$$\frac{d^2\Sigma}{d\Omega d\cos\theta'} = \frac{\alpha^2}{s} \hat{R}_{\gamma\gamma}(\theta, \theta', \tau_0),$$

$$\hat{R}_{\gamma\gamma}(\theta, \theta', \tau_0) = \left(3 \sum_f Q_f^4\right) \frac{C(s)}{4} K(\theta, \theta') I(\hat{v}, \tau_0), \quad (3.10)$$

$$I(\hat{v}, \tau_0) = \left[\frac{3\hat{v}^2 - 86\hat{v} - 61}{24(1+\hat{v})^2} + \ln \frac{1-\hat{v}}{\tau_0(1+\hat{v})} - \frac{2\tau_0}{1-\hat{v}^2} \right. \\ \left. - \frac{\tau_0^2}{8} + \frac{2\sqrt{\tau_0(\tau_0+6)}}{3(1-\hat{v}^2)^{1/2}} \right] \theta\left(\frac{1-\tau_0}{1+\tau_0} - \hat{v}\right),$$

$$\hat{v} = \left| \cos\left(\frac{\theta+\theta'}{2}\right) / \cos\left(\frac{\theta-\theta'}{2}\right) \right|.$$

As pointed out by Basham *et al.*, we can get rid of the confinement corrections by defining the following asymmetry. We consider the energy correlator, of solid angle $d\Omega$, is in the direction defined by the angle θ ; and the other one has a solid angle $d\Omega'$, the angle between the two calorimeters being

χ . An integration over the azimuthal angle is assumed. This situation is illustrated in Fig. 2. In our case (without the confinement corrections) this configuration allows for two possibilities: $\theta' = \chi - \theta$ and $\theta' = 2\pi - \theta - \chi$. The corresponding energy correlation is then

$$\bar{R}_{\gamma\gamma}(\theta, \chi, \xi_0) = R_{\gamma\gamma}(\theta, \chi - \theta, \xi_0) + R_{\gamma\gamma}(\theta, -\chi - \theta, \xi_0). \quad (3.11)$$

An analogous expression holds for $\hat{R}_{\gamma\gamma}(\theta, \chi, \tau_0)$.

Now, one defines the asymmetry of this energy correlation about $\chi = \pi/2$,

$$D_{\gamma\gamma}(\theta, \chi, \xi_0) = \bar{R}_{\gamma\gamma}(\theta, \pi - \chi, \xi_0) - \bar{R}_{\gamma\gamma}(\theta, \chi, \xi_0), \quad (3.12)$$

and analogously for $\hat{D}_{\gamma\gamma}(\theta, \chi, \tau_0)$. The usefulness of this asymmetry comes from the fact that the leading confinement corrections, of order $\langle p_T \rangle / \sqrt{s}$, do not contribute to $D(\theta, \chi, \xi_0)$, since they are symmetric¹ under the interchange $\chi \rightarrow \pi - \chi$. Only the confinement corrections of order $\langle p_T \rangle^2 / s$ could affect the free-quark calculation. We will neglect these corrections.

In terms of θ and χ the function $K(\theta, \theta')$, defined in Eq. (3.7) reads

$$K(\theta, \chi) = \frac{1}{\sin^6(\chi/2)} \frac{1+z^2(\theta, \chi)}{[1-z^2(\theta, \chi)]^2}, \quad (3.13)$$

with

$$\hat{v} = \left| \frac{\cos(\chi/2)}{\cos(\theta - \chi/2)} \right|, \quad z = \frac{\sin(\theta - \chi/2)}{\sin(\chi/2)}. \quad (3.14)$$

From these expressions and from Eqs. (3.8)–(3.12) one can easily realize that the energy correlations $\bar{R}_{\gamma\gamma}(\theta, \chi, \xi_0)$ and $\hat{R}_{\gamma\gamma}(\theta, \chi, \xi_0)$ can be strongly asymmetric under the exchange $\chi \rightarrow \pi - \chi$, which corresponds to the interchange $\sin\chi/2 \rightarrow \cos\chi/2$, $\sin(\theta - \chi/2) \rightarrow \cos(\theta - \chi/2)$. Therefore, the asymmetries $D_{\gamma\gamma}(\theta, \chi, \xi_0)$ and $\hat{D}_{\gamma\gamma}(\theta, \chi, \tau_0)$ are expected to be important.

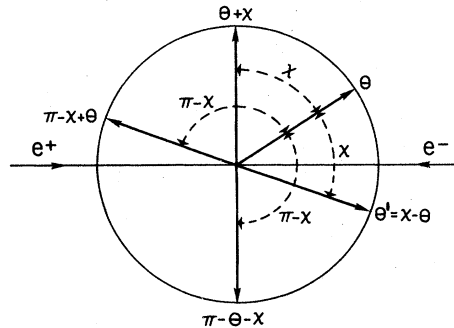


FIG. 2. Illustration of the angles θ , θ' , and χ which appear in the definition of the energy correlation (see text).

In comparing these asymmetries in $\gamma\gamma$ processes with that predicted from QCD radiative corrections to the one-photon contribution, we will be particularly interested in the case $\theta = \pi/2$, for which the expressions (3.13) and (3.14) become simpler, namely,

$$K(\pi/2, \chi) = \frac{1}{\sin^4(\chi/2) \cos^2\chi},$$

$$\hat{v}(\pi/2, \chi) = |\cot(\chi/2)|. \quad (3.15)$$

In Sec. VII we discuss the possibility of studying $\gamma\gamma$ processes from the energy correlation as a function of the hadronic invariant mass $M_H = \sqrt{\tau s}$. The contribution of light quarks to the differential energy correlation is

$$\frac{d^3\Sigma}{d\sqrt{\tau} d\Omega d\cos\theta'} = \frac{\alpha^2}{s} r_{\gamma\gamma}(\tau, \theta, \chi),$$

$$r_{\gamma\gamma}(\tau, \theta, \chi) = \left(3 \sum_f Q_f^4\right) \frac{C(s)}{2} K(\theta, \chi) \times \frac{1}{\sqrt{\tau}} H\left(\left(\frac{\tau}{1-\hat{v}^2}\right)^{1/2}, \hat{v}\right) \theta\left(\frac{1-\tau}{1+\tau} - \hat{v}\right). \quad (3.16)$$

IV. COMPARISON BETWEEN THE CONTRIBUTIONS FROM 2γ PROCESSES AND QCD CORRECTIONS TO THE ANTENNA PATTERN AND TO THE ENERGY CORRELATION

In e^+e^- collisions, the energy pattern and the energy correlation of the hadronic final states acquire contributions essentially from two different processes, corresponding to the production of hadronic energy either through one virtual photon or through two-quasireal-photon collisions. The second contribution cannot be completely disentangled from the one-photon processes since the additional e^+e^- pair are almost collinear to the colliding beams and are not tagged in most current experiments. In two-photon processes the total energy and the final hadronic invariant mass are both less than \sqrt{s} . The $\gamma\gamma$ induced events can then be suppressed by asking for data with either one or the other of these quantities being as near as possible to their maximum value. But they cannot be completely eliminated and it is important to know how large they should be for a given experimental setup.

When discussing the one-photon contribution to the antenna pattern we shall separate it in several terms, so establishing a sort of hierarchy, according to their dynamical origin. Indeed, even if all these terms contribute together with two-

photon processes to the measured antenna pattern, they all have characteristic energy dependences and angular distributions, so that one can, in principle, study each one by varying the experimental conditions.

A. Antenna pattern

The antenna pattern in e^+e^- collisions can then be written as

$$\frac{d\Sigma}{d\Omega} = \frac{\alpha^2}{s} A(s, \theta),$$

$$A(s, \theta) = A_0(s, \theta) + A_{Q\bar{Q}}(s, \theta) + A_{QCD}(s, \theta) + A_{\gamma\gamma}(s, \theta). \quad (4.1)$$

The contribution from $e^+e^- \rightarrow \gamma\gamma \rightarrow q\bar{q}$ to order $(\alpha_s)^0$ is given by

$$A_0(s, \theta) = \frac{1}{4} \left(3 \sum_f Q_f^4\right) \times \left[(1 + \cos^2\theta) + \frac{\pi C\langle p_T \rangle}{4\sqrt{s}} (1 - 3\cos^2\theta) \right], \quad (4.2)$$

where the first term corresponds to the $(1 + \cos^2\theta)$ dependence obtained in the "naive" calculations (i.e., with ultrarelativistic free quarks), while the second term gives the correction from the confinement of quarks as evaluated by Basham *et al.*¹

The second contribution to Eq. (4.1), $A_{Q\bar{Q}}$, contains the corrections which are needed in Eq. (4.2) when the final quarks in the processes $e^+e^- \rightarrow \gamma \rightarrow \bar{Q}Q$ are heavy quarks. The calculation of $A_{Q\bar{Q}}$ is presented in Appendix D and results in the expressions:

$$A_{Q\bar{Q}}(s, \theta) = \frac{3Q^2}{4} \left[\frac{\beta}{2} (1 + \beta^2) - 1 + \frac{(1 - \beta^2)^2}{2} \tanh^{-1}\beta \right] \times (1 + \cos^2\theta) + A_{m_Q}(s, \theta),$$

$$A_{m_Q}(s, \theta) = \frac{3Q^2}{4} [2\beta(1 - \beta^2) - (1 - \beta^2)^2 \tanh^{-1}\beta] \times (1 - \cos^2\theta), \quad (4.3)$$

$$\beta = \left(\frac{s - 4m_Q^2}{s} \right)^{1/2}.$$

As a matter of fact, Eq. (4.3) is just a good approximation to the exact result, which is given in Appendix D.

In the plots presented hereunder we will prefer to include the term with the $(1 + \cos^2\theta)$ angular dependence in the contribution given by Eq. (4.2). In this way, the other term, $A_{m_Q}(s, \theta)$ can be more

easily compared with the other contributions.

The QCD corrections to order α_s consist of the emission of real and virtual gluons. They have been evaluated by Basham *et al.*,¹ who obtain

$$A_{\text{QCD}} = \frac{\alpha_s(s)}{2\pi} (1 - \cos^2\theta). \quad (4.4)$$

The contribution from $\gamma\gamma$ processes to the antenna pattern, $A_{\gamma\gamma}(s, \theta)$, has been studied in Sec. II. It depends on the experimental cuts on the data. We have considered two typical situations. In case (a), where only events with total hadronic invariant mass, M_H , larger than some value $(\tau_0 s)^{1/2}$ are selected, $A_{\gamma\gamma}(s, \theta)$ is given by Eq. (2.18). Conversely, in the experimental situation (b), where only the total hadronic energy (in the e^+e^- c.m. system) is required to be larger than a given value $\zeta_0 \sqrt{s}$ ($\zeta_0 > \frac{1}{2}$), one should take $A_{\gamma\gamma}(s, \theta)$ from Eq. (2.16). Both of these expressions are improved by adding the corrections from the confinement of quarks, which are estimated in Appendix A.

All these contributions to the antenna pattern, including the confinement corrections, are plotted together in Fig. 3 for $\sqrt{s} = 30$ GeV and five flavors, and, in Fig. 4, for $\sqrt{s} = 100$ GeV and six flavors. For other values of \sqrt{s} , one can easily extrapolate these curves from their s dependence given in Eqs. (4.2)–(4.5).

The relevant contribution from $\gamma\gamma$ processes appears in the small-angle region, while the QCD corrections are more manifest at large angles. However, disentangling these contributions

from the dominant $(1 + \cos^2\theta)$ term should be a difficult task unless one can efficiently depress the $\gamma\gamma$ contribution by cutting the data. This could be done in two ways, in correspondence with the two experimental situations discussed before:

(a) Either one selects only events with invariant hadronic mass larger than $\sim 60\%$ of its maximum value \sqrt{s} (such that $\tau_0 \geq 0.3$).

(b) Or one removes all the events with total hadronic energy (in the e^+e^- c.m. system) less than $60\text{--}70\%$ of \sqrt{s} .

In both cases one should only consider the antenna pattern for $\theta \geq 30^\circ$ in order to be sure that the 2γ contamination can be safely neglected.

A conclusion which we would like to stress is that, interestingly enough, the simpler experiments of type (b) look more efficient to eliminate the $\gamma\gamma$ processes. This seems nice since they are more in the spirit of the calorimeter experiments discussed in this work.

Another aspect one has to pay attention to, are the corrections to be made in the presence of heavy quarks. Therefore, it is worth stressing that the corrections due to massive quarks are calculable (at least outside the resonance regions) to a good approximation, as shown in Appendix D. They have a characteristic energy behavior which, in principle, could be used to separate them from the QCD corrections.

Only the one-photon contribution to the annihilation channel is shown in the figures. In this case, the ratio $A_{\gamma\gamma}/A_0$ grows like $\ln^2 s$, while A_{QCD}/A_0 goes down as $\ln^{-1} s$. For $\sqrt{s} > M_Z$, the weak inter-

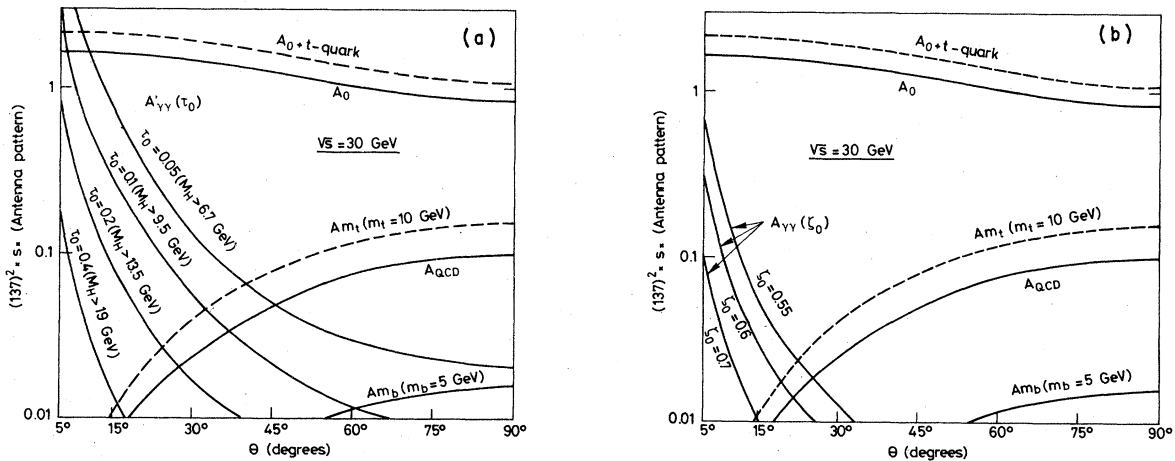


FIG. 3. (a) Important contributions to the antenna pattern in e^+e^- collisions at $\sqrt{s} = 30$ GeV with five flavors. A_0 is the contribution from annihilation (corrected for confinement), A_{QCD} is the QCD radiative correction to A_0 (at order α_s), and $A_{\gamma\gamma}$ is the background from $\gamma\gamma$ collisions, for several choices of the cutoff on the hadronic invariant mass M_H . The dashed lines are the eventual contributions of a quark t with $m_t = 10$ GeV. (b) Same as (a) with a $\gamma\gamma$ background ($A_{\gamma\gamma}$) for several cutoffs in the total hadronic energy E_H .

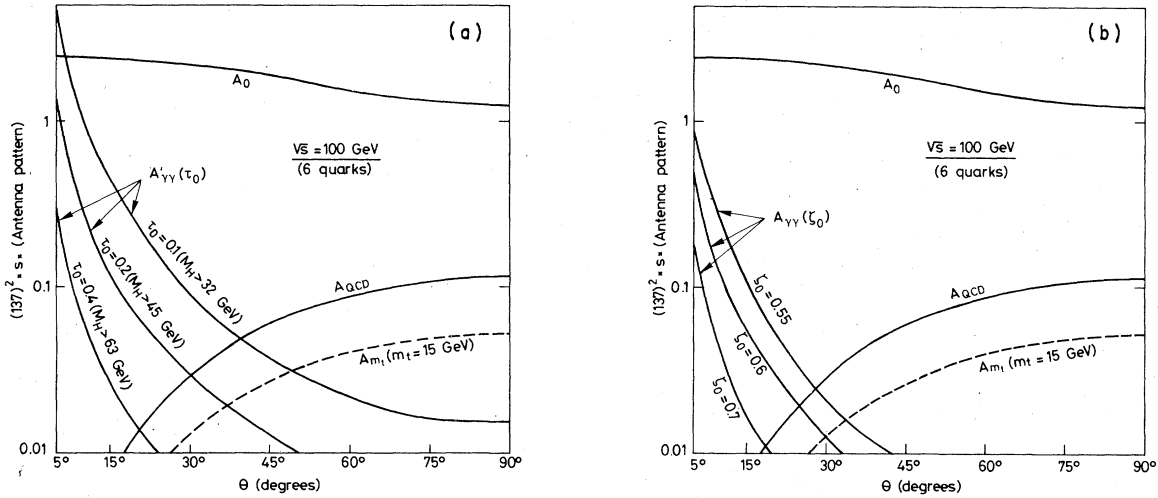


FIG. 4. (a) Same as Fig. 3(a) for $\sqrt{s}=100$ GeV, with six flavors. (b) Same as Fig. 3(b) for $\sqrt{s}=100$ GeV, six flavors.

actions become sizable, and both A_0 and A_{QCD} are increased by a numerical factor of $O(1)$, outside the Z^0 pole. This factor would be of $O(1/\alpha) \sim 100$ on the top of the Z^0 pole, $\sqrt{s} = M_Z 0$, where the 2γ background should be negligible. However, an experimental determination of the s dependence of the antenna pattern is always necessary in order to eliminate the effects from heavy-quark masses and decay.

B. Energy correlation

We now turn our attention to the asymmetry in the energy correlation, which we divide into three main contributions as follows:

$$\int_0^{2\pi} d\phi' \left[\frac{d^2\Sigma}{d\Omega d\Omega'}(\theta, \pi - \chi) - \frac{d^2\Sigma}{d\Omega d\Omega'}(\theta, \chi) \right] = \frac{\alpha^2}{s} [D_0(\theta, \chi) + D_{\text{QCD}}(\theta, \chi) + D_{\gamma\gamma}(\theta, \chi)], \quad (4.5)$$

where θ is the angle between the first calorimeter and the positron beam, while χ is the angle between the calorimeters. We have integrated over the azimuthal angle between the calorimeters in order to eliminate the effect of both the quark confinement and the QCD corrections on the azimuthal dependence.

The first term in Eq. (4.5), $D_0(\theta, \chi)$, is defined as the contribution to the energy correlation from $e^+e^- \rightarrow \gamma\gamma + \bar{q}q$, to order α_s^0 , i.e., without QCD radiative corrections. In the limit where the quark confinement is neglected, this term vanishes, since the energy correlation becomes trivially proportional to the sum of two δ functions. The confinement corrections of order $\langle p_T \rangle / \sqrt{s}$ will produce some smearing of the δ functions but

the result remains symmetric under $\chi \rightarrow \pi - \chi$. It is easy to realize that the confinement corrections of order $\langle p_T \rangle^2 / s$ could introduce some asymmetry in the energy correlation. Therefore, $D_0(\theta, \chi)$ is proportional to $\langle p_T \rangle^2 / s$ and can be neglected at very high energies.

The second term in Eq. (4.5), $D_{\text{QCD}}(\theta, \chi)$ comes from the QCD radiative corrections. It has been calculated in Ref. 1 to order α_s (gluon emission and virtual-gluon exchange).

The last term in Eq. (4.5), $D_{\gamma\gamma}(\chi, \theta)$, is the asymmetry in the energy correlation for $\gamma\gamma$ processes, which has been discussed in Sec. III. According to the characteristics of the experimental setup, the events should be selected in a manner consistent with one of the criteria, (a) or (b), discussed in Secs. II and III. The asymmetry $D_{\gamma\gamma}(\chi, \theta)$ will then be given by Eqs. (3.11) and (3.12), respectively, supplied with Eq. (3.10) or Eq. (3.8).

Typical predictions for the contributions to the energy correlation asymmetry, Eq. (4.5), are shown in Figs. 5 and 6. These numerical results can be easily understood from the fact that 2γ -originated events are concentrated at small angles. If the angle θ is fixed, which means that one jet comes out around this direction, then the other jet will tend to be produced as near the forward direction as allowed by the kinematical constraints, that are essentially given by the θ functions in Eqs. (3.8) and (3.10). This explains the existence of a peak in $D_{\gamma\gamma}(\theta, \chi)$, followed by an abrupt decrease, which occurs very near to the point (defined by the θ functions)

$$\tan\left(\frac{\theta - \chi}{2}\right) = \tau_0 \tan\left(\frac{\theta}{2}\right)$$

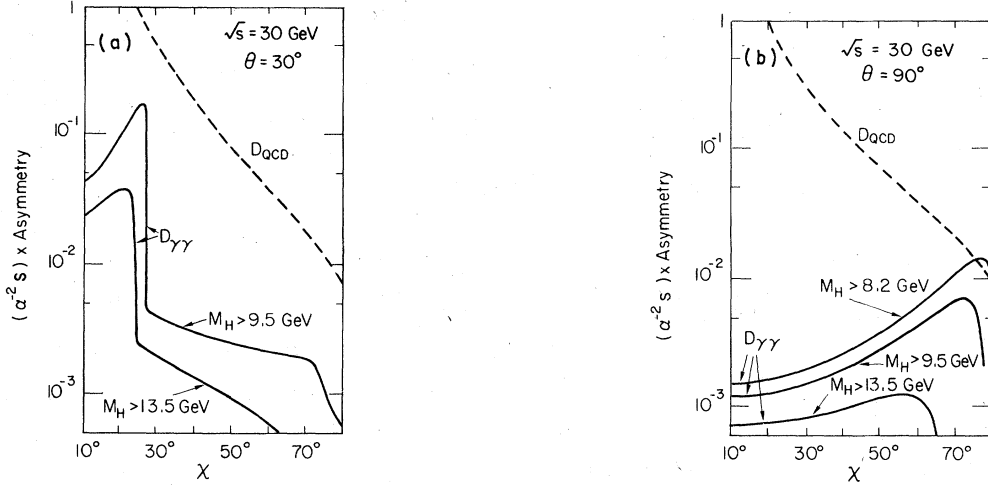


FIG. 5. (a) Asymmetry in the energy correlation (see text) for $\gamma\gamma$ initiated events for several cutoffs in the hadronic invariant mass M_H , at $\sqrt{s} = 30$ GeV, and $\theta = 30^\circ$. The dashed line is the corresponding QCD asymmetry (Ref. 1) for the annihilation channel ($e^+e^- \rightarrow$ hadrons). (b) Same as (a), but at $\theta = 90^\circ$.

for a fixed value of τ_0 [$\tau_0 = (2\xi_0 - 1)$ in case (b)]. This pattern of the energy correlation asymmetry is a general, but very characteristic, property of $\gamma\gamma$ collisions. The steepest part of $D_{\gamma\gamma}(\theta, \chi)$ could be more affected by confinement corrections [of $O(\langle p_T^2 \rangle / M_H^2)$] and QCD radiative corrections, but its general trend should remain.

In general, the $\gamma\gamma$ background in measurements of D_{QCD} should be relatively small for $\theta > 30^\circ$. Experimental cuts like $M_H > 0.4\sqrt{s}$ or $E_H > 0.6\sqrt{s}$ are enough to reduce the 2γ contribution to a reasonable amount. At $\theta = 90^\circ$, where D_{QCD} is maximum and mostly easily measurable, $D_{\gamma\gamma}$ is essentially flat in χ and rather small in magnitude.

V. CONTRIBUTION OF NARROW BOUND STATES TO THE ANTENNA PATTERN AND TO THE ENERGY CORRELATION

In this section we evaluate the antenna pattern and the energy correlation from the formation of bound states of heavy quarks^{11,12} in $\gamma\gamma$ collisions (as b and t quarks), below the threshold for the production of new-flavored mesons. These are narrow states which mostly decay into two gluons, since the bound states produced by the two-photon system have to be even under charge conjugation.

Here we shall take into account only the S and P waves, the D waves giving a much smaller con-

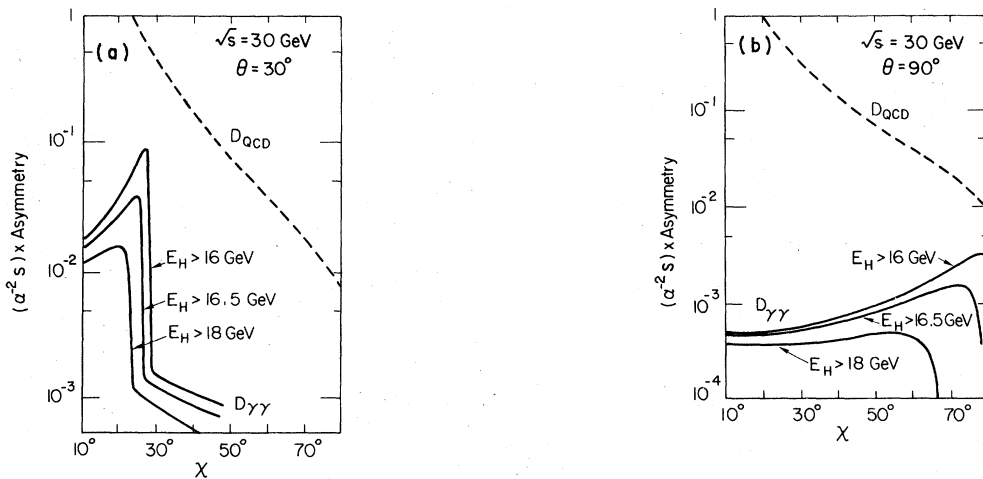


FIG. 6. (a) Same as Fig. 5(a), but for several cutoffs in the total hadronic energy, E_H , at $\theta = 30^\circ$. (b) Same as (a), but at $\theta = 90^\circ$.

tribution to the cross section. The C -even P waves (1^{++}) do not couple to two real photons so that they do not contribute in the EPA. So we remain with the 0^{++} , 0^{-+} , and 2^{++} states.

In the narrow-width approximation, the contribution of the spin-zero states to the $2\gamma \rightarrow 2$ gluons cross section is

$$\frac{d\hat{\sigma}^{(0^{++})}}{d\Omega^*} = 2\pi \sum_n \frac{\Gamma_{n \rightarrow \gamma\gamma}^{0^{++}}}{M_n} \delta(\tau_s - M_n^2), \quad (5.1)$$

where we have summed over all the radially excited bound states below the threshold.

In the nonrelativistic limit, which is hopefully good for such a heavy quark, the 2^{++} state couples to two real gluons (or photons) only with helicity ± 2 .¹³ Under this assumption the contribution of the 2^{++} states to the $2\gamma \rightarrow 2$ gluons cross section in the narrow-width approximation is

$$\frac{d\hat{\sigma}^{(2^{++})}}{d\Omega^*} = \frac{25\pi}{8} \sum_n \frac{\Gamma_{n \rightarrow \gamma\gamma}^{2^{++}}}{M_n} \delta(\tau_s - M_n^2) \times (\cos^4\theta^* + 6\cos^2\theta^* + 1). \quad (5.2)$$

We introduce the notation

$$\gamma(J^{PC}) = \sum_n \frac{\Gamma_{n \rightarrow \gamma\gamma}^{J^{PC}}}{\alpha^2 M_n^2}. \quad (5.3)$$

The cross sections (5.1) and (5.2) become then proportional to the dynamical factors (5.3), which depend on the quarkonium wave functions at the origin and their derivatives. A determination of $\gamma(0^{++})$ which does not assume any specific form

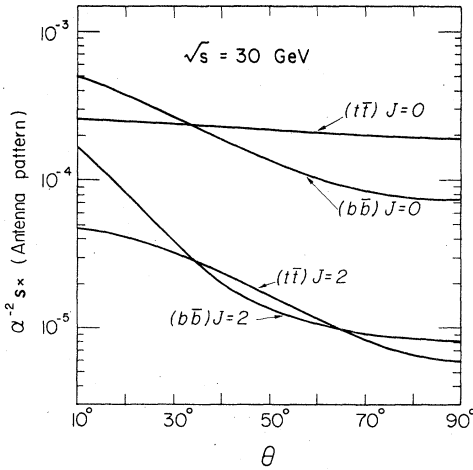


FIG. 7. Energy pattern from C -even bound states produced in $\gamma\gamma$ collisions [see Fig. 9(h)]. The contributions from $J=0$ and $J=2$ states are shown separately for $(b\bar{b})$ bound states ($m_b = 5$ GeV) and $(t\bar{t})$ ones ($m_t = 10$ GeV). The e^+e^- c.m. energy is $\sqrt{s} = 30$ GeV.

of the potential is provided by the WKB sum rules. This method is described in detail in Ref. 12. In this approach, the overall contribution of the 0^{++} states is given by (in the case of a quark of charge $\frac{2}{3}$)

$$\gamma(0^{++}) = \frac{16\sqrt{2}}{27\pi} \left(\frac{\Delta}{2m_Q}\right)^{3/2} \int_0^1 dx \frac{\sqrt{x}}{(1 + \Delta x/2m_Q)^3}, \quad (5.4)$$

where Δ is the gap between the first bound state and the threshold for flavor production. For $m_Q = m_t \sim 10$ GeV one expects a gap $1 < \Delta < 2$ GeV, so that, Eq. (5.4) gives

$$2 \times 10^{-3} \lesssim \gamma(0^{++}) \lesssim 5 \times 10^{-3}.$$

A. Antenna pattern

From Eqs. (5.1), (5.2), and (5.3) one gets for the contribution of the bound states to the antenna pattern in the $\gamma\gamma$ c.m. system:

$$\frac{d\hat{\Sigma}^{(0^{++})}}{d\Omega^*} = \frac{\alpha^2}{s} (2\pi)\gamma(0^{++})\delta\left(\tau - \frac{4m_Q^2}{s}\right), \quad (5.5)$$

$$\frac{d\hat{\Sigma}^{(2^{++})}}{d\Omega^*} = \frac{\alpha^2}{s} \left(\frac{25\pi}{8}\right)\gamma(2^{++})\delta\left(\tau - \frac{4m_Q^2}{s}\right) \times (\cos^4\theta^* + 6\cos^2\theta^* + 1).$$

Introducing Eq. (5.5) into Eq. (2.9a) one obtains for the antenna pattern in the e^+e^- c.m. system from the bound states

$$\frac{d\Sigma^{(J^{PC})}}{d\Omega} = \frac{\alpha^2}{s} A^{(J^{PC})}(\theta),$$

$$A^{(0^{\pm+})}(\theta) = 2\pi C(s)\gamma(0^{\pm+}) \times \frac{1}{\sqrt{\tau_R}} \int_{-v_R}^{v_R} dv \frac{\tilde{H}(\tau_R, v)}{(1 - v \cos\theta)^3}, \quad (5.6)$$

$$A^{(2^{++})}(\theta) = \frac{25\pi}{8} C(s)\gamma(2^{++}) \frac{1}{\sqrt{\tau_R}} \times \int_{-v_R}^{v_R} dv \tilde{H}(\tau_R, v) \frac{z^4(\theta, v) + 6z^2(\theta, v) + 1}{(1 - v \cos\theta)^3},$$

$$\tau_R \cong (4m_Q^2/s), \quad v_R = \frac{1 - \tau_R}{1 + \tau_R}, \quad z(\theta, v) = \frac{\cos\theta - v}{1 - v \cos\theta},$$

where $\tilde{H}(\tau_R, v)$ is given by Eq. (2.18) with $\tau = \tau_R$.

The overall antenna pattern, resulting from the addition of the three terms in Eq. (5.6), with the $\gamma(J^{PC})$ factors given by a harmonic-oscillator model with frequency estimated from the $\psi' - \psi$ splitting, is shown in Figs. 7 and 8. Since the angular dependence of the bound-state contribution to the antenna pattern is much flatter than that for the $\gamma\gamma \rightarrow q\bar{q}$ processes, we could be inclined to study the C -even bound states from their contribution to the antenna pattern at large angles. In order to check this possibility, we compare Eq. (5.6) with

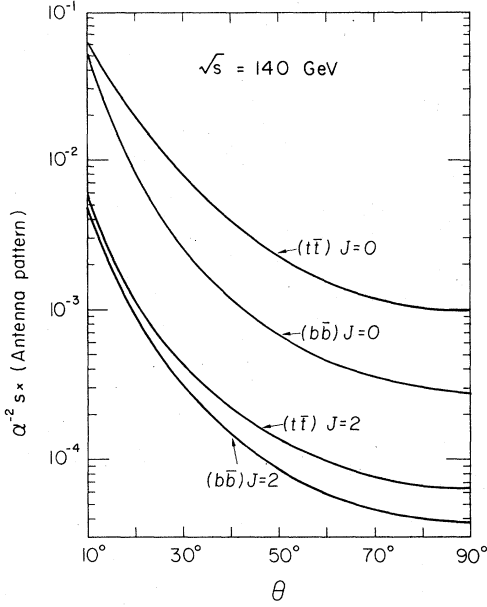


FIG. 8: Same as Fig. 7, but at $\sqrt{s} = 140$ GeV.

the antenna pattern of the lighter quarks, given by Eq. (2.20), at $\theta = \pi/2$. We call δ the experimental resolution in the hadronic mass $M_H \sim (\tau_R s)^{1/2}$, and we keep just the 0^{-+} states which give the dominant contribution. We find for the ratio between the contribution from the bound states and that from the lighter quarks,

$$\frac{A^{(0^{-+})}(\pi/2)}{\delta a(\tau_R, \pi/2)} = \frac{\pi \gamma(0^{-+}) \sqrt{\tau_R}}{3\delta (\sum_f Q_f^4) [2\rho(\tau_R) - 1]},$$

where

$$\rho(\tau_R) = \int_{-v_R}^{v_R} dv \frac{\tilde{H}(\tau_R, v)}{1-v^2} \bigg/ \int_{-v_R}^{v_R} dv \tilde{H}(\tau_R, v) > 1. \quad (5.7)$$

Assuming that N -quark doublets with $Q = \frac{2}{3}$ and $Q = -\frac{1}{3}$ are contributing to $a_{\gamma\gamma}$, and approximating $\gamma(0^{-+})$ by the WKB sum rule, Eq. (5.4), we estimate

$$\frac{\kappa}{\delta} \equiv \frac{\pi \gamma(0^{-+}) \sqrt{\tau_R}}{\delta (3 \sum_f Q_f^4)} \approx \frac{1}{\delta} \left(\frac{\Delta^3}{2m_Q s} \right)^{1/2} < \frac{1}{\delta} \left(\frac{\Delta}{2m_Q} \right)^{3/2}, \quad (5.8)$$

so that measuring the antenna pattern from bound states would require an experimental resolution $\delta \ll (\Delta/2m_Q)^{3/2}$. This could hardly be obtained for a quark mass $m_Q \gtrsim 10$ GeV, and a gap $\Delta \lesssim 2$ GeV. We conclude that the antenna pattern from the C -even bound states is too small to be measurable at this time.

B. Energy correlation

The contributions of the bound states to the energy correlation in the $\gamma\gamma$ c.m. system, which are obtained from Eqs. (5.1), (5.2), and (5.3), read

$$\begin{aligned} \frac{d^2 \hat{\Sigma}^{(0^{++})}}{d\Omega^* d\Omega'^*} &= \frac{\alpha^2}{s} \pi \gamma(0^{++}) \delta\left(\tau - \frac{4m_Q^2}{s}\right) \\ &\quad \times \delta(\cos\theta^* + \cos\theta'^*) \delta(\phi + \pi - \phi'), \\ \frac{d^2 \hat{\Sigma}^{(2^{++})}}{d\Omega^* d\Omega'^*} &= \frac{\alpha^2}{s} \left(\frac{25\pi}{16}\right) \gamma(2^{++}) \delta\left(\tau - \frac{4m_Q^2}{s}\right) \\ &\quad \times (\cos^4\theta^* + 6\cos^2\theta^* + 1) \\ &\quad \times \delta(\cos\theta^* + \cos\theta'^*) \delta(\phi + \pi - \phi'). \end{aligned} \quad (5.9)$$

The variables θ^* and θ'^* are related to the angles in the e^+e^- c.m. system as follows:

$$\begin{aligned} \cos\theta^* &= -\cos\theta'^* = -\sin\left(\frac{\theta - \theta'}{2}\right) \bigg/ \sin\left(\frac{\theta + \theta'}{2}\right), \\ \delta(\cos\theta^* + \cos\theta'^*) &= \frac{\sin^2\left(\frac{\theta + \theta'}{2}\right)}{2\cos^2\left(\frac{\theta - \theta'}{2}\right)} \\ &\quad \times \delta\left(v - \frac{\cos\left(\frac{\theta + \theta'}{2}\right)}{\cos\left(\frac{\theta - \theta'}{2}\right)}\right). \end{aligned} \quad (5.10)$$

Introducing Eqs. (5.9) and (5.10) into Eq. (3.3) and performing the trivial integrations on the δ functions, one finds for the energy correlation from the bound-states in the e^+e^- c.m. system, in terms of the variables θ, χ , defined in Sec. III:

$$\begin{aligned} \frac{d^2 \Sigma^{(J^{PC})}}{d\Omega d\cos\theta'} &= \frac{\alpha^2}{s} [R^{(J^{PC})}(\theta, \chi) + R^{(J^{PC})}(\theta, -\chi)], \\ R^{(0^{++})}(\theta, \chi) &= \frac{\pi \gamma(0^{++}) C(s) G(\tau_R, \theta, \chi)}{2 \sin^6(\chi/2) [1 - z^2(\theta, \chi)]}, \\ R^{(2^{++})}(\theta, \chi) &= \frac{25}{16} \frac{R^{(0^{++})}}{\gamma^{(0^{++})}} \gamma^{(2^{++})} \\ &\quad \times [z^4(\theta, \chi) + 6z^2(\theta, \chi) + 1], \end{aligned} \quad (5.11)$$

where z and \hat{v} are defined in Eq. (3.14), and,

$$G(\tau_R, \theta, \chi) = \frac{\tilde{H}(\tau_R, \hat{v})}{(1 - \hat{v}^2)^{1/2}} \theta\left(\frac{1 - \tau_R}{1 + \tau_R} - \hat{v}\right). \quad (5.12)$$

These expressions account for the global contribution of all bound states to the energy correlation in any interval of the hadronic mass that includes the resonance region. It can be useful in studying the C -even bound states only if one is able to experimentally disentangle this term from the contribution of the lighter quarks, given by Eq. (3.16). In order to test this possibility, we assume an experimental resolution δ and we consider the ratio

between the energy correlation from 0^{-+} states, which are the dominant resonances, and that from the lighter quarks. We find

$$\frac{R^{(0^{-+})}(\theta, \chi)}{\delta \gamma_{\gamma\gamma}(\tau_R, \theta, \chi)} = \frac{\kappa}{\delta} \frac{1 - z^2(\theta, \chi)}{1 + z^2(\theta, \chi)}, \quad (5.13)$$

where κ is given in Eq. (5.8). This ratio is small for any reasonable value of δ . Therefore, it would be practically impossible to measure the energy correlation from the production of C -even states in $\gamma\gamma$ processes.

VI. ANTENNA PATTERN FOR HEAVY-QUARK PRODUCTION IN TWO-PHOTON PROCESSES

The quark masses have been neglected in the calculations of Sec. II. The results there apply whenever the quark masses are very small as compared to the energy. This is always the case for light quarks, since the perturbative calculations make sense only if $\alpha_s \ll 1$, which occurs at high energies as compared to the light-quark masses. On the other hand, the quark confinement affects the free-quark calculations only by corrections of the order of $\langle p_T \rangle / \sqrt{s}$. The QCD radiative corrections are also relatively small.

For heavy quarks, whose masses are such that $\alpha_s(m_Q^2) \ll 1$, the free-quark calculations are probably reliable even at energies which are not very far from the threshold for heavy-quark production. As a consequence, one has to take care of two effects. First, the cross sections cannot be always calculated in the ultrarelativistic limit, and threshold effects have to be taken into account. Secondly, in the course of the fragmentation mechanism, most of the heavy-quark energy goes to a heavy hadron, which carries the quark flavor and so must weakly decay into light particles. The spread of the decay of the heavy hadron is of the order of m_Q / \sqrt{s} and has to be included in the calculations. A simple way to obtain the antenna pattern for heavy quarks is presented in Appendix B. It is a trivial generalization of the formalism developed in Ref. 14 and gives the partial-wave decomposition of the antenna pattern in terms of the partial waves for quark production. In Appendix C, the resulting formulas are improved through the introduction of the fragmentation functions.

We will now use this machinery in the calculation of the antenna pattern for $\gamma\gamma \rightarrow \bar{Q}Q$. The cross section for this process is given in Eq. (2.11). Its partial-wave decomposition is

$$\begin{aligned} \frac{d\hat{\sigma}^*}{d\Omega^*} &= \frac{3\alpha^2 Q^4}{\tau s} \sum_n (2n+1) E_{2n}(\beta) P_{2n}(\cos\theta^*), \\ E_0(\beta) &= (3 - \beta^4) Q_0\left(\frac{1}{\beta}\right) - \beta(2 - \beta^2), \\ E_{2n}(\beta) &= (3 - \beta^4) Q_{2n}\left(\frac{1}{\beta}\right) + 2n(1 - \beta^2) \left[Q_{2n}\left(\frac{1}{\beta}\right) - Q_{2n-1}\left(\frac{1}{\beta}\right) \right], \\ \beta &= [(s - 4m_Q^2)/s]^{1/2}, \end{aligned} \quad (6.1)$$

where $Q_n(x)$ are Legendre functions of the second kind. The antenna pattern in the $\gamma\gamma$ c.m. system is then obtained from Eq. (B6) of Appendix B:

$$\frac{d\Sigma^*}{d\Omega^*} = \frac{3\alpha^2 Q^4}{\tau s} \sum_n (2n+1) E_{2n}(\beta) R_{2n}(\beta) P_{2n}(\cos\theta^*), \quad (6.2)$$

$$R_n(\beta) = \frac{1 - \beta^2}{2\beta} Q_n^2\left(\frac{1}{\beta}\right). \quad (6.3)$$

In the $\beta \rightarrow 1$ limit, $R_n(\beta) \rightarrow 1$ and Eq. (6.2) reduces to Eq. (2.11) in this limit. Introducing Eq. (6.2) into Eq. (2.9a) one gets for the antenna pattern from $\gamma\gamma \rightarrow$ heavy quarks in the e^+e^- c.m. system:

$$\begin{aligned} \frac{d^2\Sigma}{d\sqrt{\tau} d\Omega} &= \frac{\alpha^2}{s} a_Q(\tau, \theta), \\ a_Q(\tau, \theta) &= 2(3Q^4) \frac{C(s)}{\tau} \int_{(\tau-1)/(\tau+1)}^{(1-\tau)/(1+\tau)} dv \frac{\bar{H}(\tau, v) F_Q(v, \theta)}{(1 - v \cos\theta)^3}, \\ F_Q(v, \theta) &= \sum_n (2n+1) E_{2n}(\beta) R_{2n}(\beta) P_{2n}(\cos\theta^*), \end{aligned} \quad (6.4)$$

where $\cos\theta^*$ is given by Eq. (2.4) and $\bar{H}(\tau, v)$ is defined in Eq. (2.18).

VII. CONTRIBUTIONS FROM THE QCD STRUCTURE OF THE PHOTON

Until now, only the process $\gamma\gamma \rightarrow q\bar{q}$ of Fig. 9(a) has been considered. Radiative corrections from gluon emission, have also to be considered. For instance, the process in Fig. 9(b) where a quark is produced at large angle and almost on-shell, and then it radiates a very collinear gluon. This kind of correction is interesting because it can be a source of mass singularities. The antenna pattern is defined in order to be free of these singularities. Virtual and real gluon emission should only introduce corrections of the order of $[\alpha_s(s)/\pi]$, which are being neglected in this work. However, processes like those of Fig. 9(c), where one photon has a deep-inelastic collision with a constituent (quark or gluon) of the other, have to be taken into account. Indeed, Witten⁹ obtained the remarkable result that the leading contributions to the photon structure functions can be exactly calculated in QCD. More recently, several authors⁹ have derived the same result by using differ-

ent techniques. This can be most easily interpreted as follows. The momentum distributions of quarks $G_{q/\gamma}(x, Q^2)$ [and gluons $G_{g/\gamma}(x, Q^2)$] inside the real photon is essentially known (at large Q^2). Interestingly enough, they are proportional to $[\alpha_s(Q^2)]^{-1}$. One of these constituents can have a large-momentum-transfer strong interaction (Q^2 large), whose rate is proportional to $\alpha_s(Q^2)$. The α_s^{-1} factor in the structure function then cancels the α_s factor in the interaction and the final result is independent of $\alpha_s(Q^2)$.

We now proceed to calculate the contribution of this kind of processes, due to the QCD structure functions of the photon, to the antenna pattern. First of all we notice that the gluon distributions $G_{g/\gamma}(x, Q^2)$ are relatively small⁹ and can be neglected in a first approximation. Then, we remark that this kind of $\gamma\gamma$ interaction will produce three hadronic jets in the final state [one gluon + one quark + photon fragments, in Fig. 9(c)]. Since the fragments go either forward or backward, we shall not include them in the final hadronic energy and invariant mass, which are assumed to be measured outside the beam direction. With this choice, only the energy carried by the initial constituent, a quark in Fig. 9(c), is important. Since we know the equivalent-photon content of an incident electron $N(x)$ given by Eq. (2.2) (due to the QED structure of the electron), as well as the quark distribution in the real photon $G_{q/\gamma}(x, Q^2)$ (due to the QCD structure of the photon), we can calculate the quark structure function of the electron.¹⁰ The result is

$$G_{q/e}(x, Q^2) = C^{1/2}(s) \frac{\alpha Q_i^2}{\alpha_s(Q^2)} q(x), \quad (7.1)$$

$$q(x) = \frac{(1-x)\bar{f}(x)}{4\pi}, \quad (7.2)$$

where $C(s)$ is given in Eq. (2.10) and $\bar{f}(x)$ is plotted in Fig. 1 of Ref. 10. This is to be compared to the photon momentum distribution in the electron as defined in the EPA [cf. Eq. (2.2)]

$$N(x) = C^{1/2}(s)h(x), \quad (7.3)$$

$$h(x) = \frac{1+(1-x)^2}{2}. \quad (7.4)$$

The antenna pattern of the processes in Fig. 9(c) can be now easily obtained from the analogous one of Eq. (2.6) with one of the photon distributions, $N(x_i)$ ($i=1, 2$), replaced by $G_{q/e}(x_i, Q^2)$. The antenna pattern for $q\gamma \rightarrow qG$ in the $(q\gamma)$ c.m. system is,

$$\frac{d\hat{\Sigma}^\sigma}{d\Omega^*} = \frac{\alpha\alpha_s(Q^2)}{\tau s} \left(3 \sum_f Q_f^2 \right) \frac{1}{3} \left(\frac{4}{\sin^2\theta^*} + 2 \right). \quad (7.5)$$

The kinematics here is exactly the same as in Sec. II. In particular the relations given in Eq. (2.3) remain unchanged. Notice again that the factor $\alpha_s(Q^2)$ in the numerator of Eq. (7.5) will balance the same factor in the denominator of Eq. (7.1), so that the resulting antenna pattern is independent from $\alpha_s(Q^2)$. This is to be contrasted with the radiative corrections, like the gluon emission in Fig. 9(b).

From Eqs. (2.9a), (2.4), (2.3), (7.1)–(7.5), one finally obtains for the antenna pattern of the processes which we are considering here, as a function of the hadronic invariant mass, $M_H = (\tau s)^{1/2}$:

$$\begin{aligned} \frac{d\Sigma^\sigma}{d\Omega d\sqrt{\tau}} &= \frac{\alpha^2}{s} a_\sigma(\tau, \theta), \\ a_\sigma(\tau, \theta) &= \left(16 \sum_f Q_f^4 \right) \frac{C(s)}{\tau} \\ &\quad \times \int_0^{(1-\tau)/(1+\tau)} dv \bar{H}_q(\tau, v) F_q(v, \theta), \\ F_q(v, \theta) &= \frac{2}{(1-v^2) \sin^2\theta (1-v^2 \cos^2\theta)} \\ &\quad + \frac{1+3v^2 \cos^2\theta}{(1-v^2 \cos^2\theta)^3}, \quad (7.6) \\ \bar{H}_q(\tau, v) &= (1-v^2)^{1/2} [h(x_1)q(x_2) + h(x_2)q(x_1)], \\ x_1 &= \left(\tau \frac{1+v}{1-v} \right)^{1/2}, \quad x_2 = \left(\tau \frac{1-v}{1+v} \right)^{1/2}. \end{aligned}$$

Notice in particular the similarities between Eq. (7.6) and Eq. (2.20). For large values of $\sqrt{\tau}$ the contribution of Eq. (7.6) is an order of magnitude smaller than the antenna pattern in Eq. (2.20), since $q(x) \ll h(x)$ for $x \sim O(1)$. For very small values of \sqrt{s} , both contributions can become equally important.

As a matter of fact, there are also contributions from the hard scattering between two hadronic constituents, one from each photon. Examples are pictured in Figs. 9(e), 9(f), 9(g). However, these contributions become important only at very low values of $\sqrt{\tau}$. They will be neglected in our numerical calculations.

The antenna pattern as given by Eq. (7.6) has to be corrected for the nonperturbative effects of confinement. This can be done by following the lines of Appendix A. The final, corrected result is then obtained by replacing in Eq. (7.6):

$$F_q(v, \theta) \rightarrow F_q(v, \theta) + \frac{C(\hat{p}_T)}{\sqrt{\tau s} \sin^3\theta} F_{cc}(v, \theta), \quad (7.7)$$

where $F_{cc}(v, \theta)$ is defined in Eq. (A10).

The energy correlation for the processes in Fig. 9(c) can be evaluated from Eqs. (7.2)–(7.4) and (3.3). The calculations are analogous to those

performed in Sec. III, and the resulting expression is

$$\frac{d^3\Sigma(\theta, \theta')}{d\Omega d\cos\theta' d\sqrt{\tau}} = \frac{\alpha^2}{s} r_{\mathcal{Q}}(\tau, \theta, \chi),$$

$$r_{\mathcal{Q}}(\tau, \theta, \chi) = \left(2 \sum_f Q_f^4 \right) \frac{C(s)}{\sqrt{\tau}} H_{\mathcal{Q}}(x_1, x_2) K_{\mathcal{Q}}(\theta, \theta'),$$

$$H_{\mathcal{Q}}(x_1, x_2) = h(x_1)q(x_2) + q(x_1)h(x_2),$$

$$K_{\mathcal{Q}}(\theta, \theta') = \frac{1}{\sin^4\left(\frac{\theta + \theta'}{2}\right)}$$

$$\times \frac{3 \sin^2\left(\frac{\theta + \theta'}{2}\right) - \sin^2\left(\frac{\theta - \theta'}{2}\right)}{\left[\sin^2\left(\frac{\theta + \theta'}{2}\right) - \sin^2\left(\frac{\theta - \theta'}{2}\right) \right]^2},$$

$$x_1 = \sqrt{\tau} \left(\frac{1-v}{1+v} \right)^{1/2}, \quad x_2 = \frac{\tau}{x_1} = \sqrt{\tau} \left(\frac{1+v}{1-v} \right)^{1/2}$$

$$v = \left| \frac{\cos\left(\frac{\theta + \theta'}{2}\right)}{\cos\left(\frac{\theta - \theta'}{2}\right)} \right|.$$

Before ending this section, we would like to comment on the validity of the photon structure functions in Eq. (7.1). This is the leading term in the $Q^2 \rightarrow \infty$ limit, being proportional to $1/\alpha_s(Q^2)$. For finite values of Q^2 , one has to take care of three kinds of corrections to Eq. (7.1): (i) next-to-the-leading-order terms, of $O(\ln\alpha_s(Q^2))$, $O(1)$, \dots ,¹⁵ (ii) corrections due to the quark masses, in particular, for heavy quarks,¹⁶ and (iii) contributions to the γ structure functions from hadronic resonances.

Corrections of types (i) and (ii) are in principle computable in QCD. Once they are known, they can be easily included in our calculations by introducing the corrected quark distributions in place of Eq. (7.1). The corrections of type (iii) have been discussed by Witten.⁹

As a matter of fact, the $\gamma\gamma$ processes at large M_H/\sqrt{s} give interesting information on the photon structure functions at large x , where the QCD predictions mostly disagree with a naive QED calculation.⁹ In this region the corrections from hadronic resonances are expected to be rather small, while the computable corrections [types (i) and (ii) above] could be more relevant.

VIII. NUMERICAL ANALYSIS OF THE ANTENNA PATTERN IN $\gamma\gamma$ COLLISIONS

The results obtained from Eqs. (2.20) and (7.6) are shown in Figs. 10–17, for $\sqrt{s} = 30$ and 100 GeV. Confinement corrections have been included

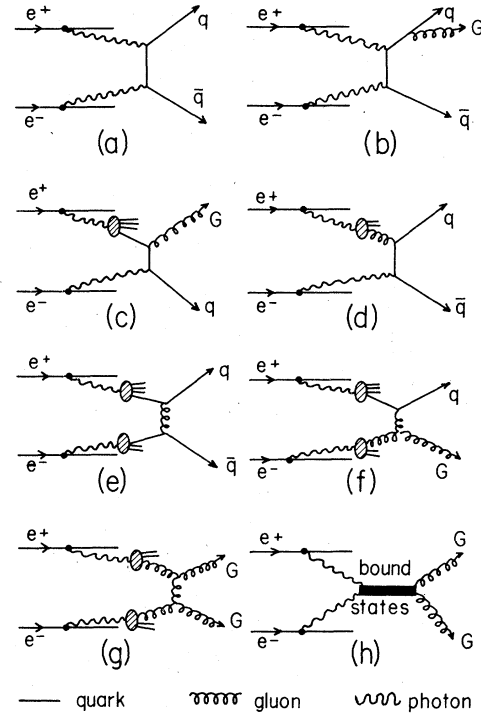


FIG. 9. Dominant processes in $e^+e^- \rightarrow e^+e^- + 2 \text{ jets} + \dots$: (a), QED diagram for quark-production; (b), QCD radiative correction to the graph (a); (c)–(d), contribution from the QCD structure function of one photon; (e)–(g), typical interactions between the constituents of the photons (the blobs represent the QCD structure functions of the real-photon; the photon fragments come out essentially along the beam direction); (h) formation of C -even bound states which mostly decay into two gluons.

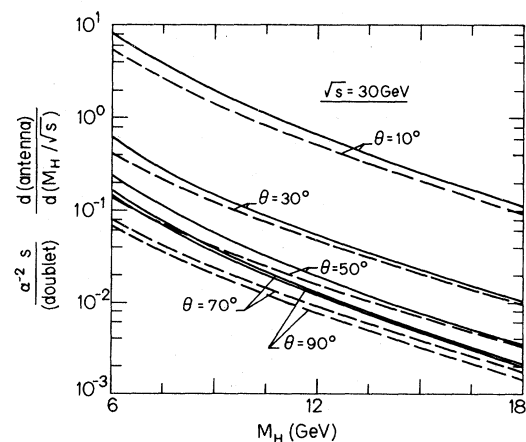


FIG. 10. The antenna pattern from the process in Fig. 9(a), as a function of M_H at typical values of θ and $\sqrt{s} = 30$ GeV. The curves are the contribution from a single doublet (a $Q = \frac{2}{3}$ quark plus a $Q = -\frac{1}{3}$ one). The results of our calculations are shown both before (dashed lines) and after (solid lines) confinement corrections are taken into account.

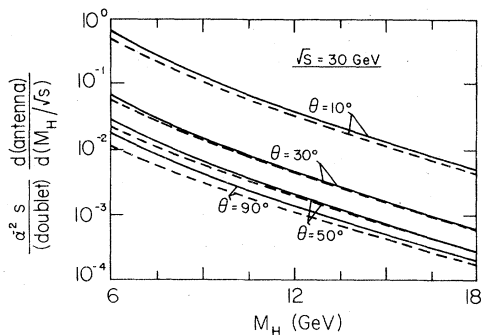


FIG. 11. Same as Fig. 10 for the process in Fig. 9(c). The overall antenna pattern is essentially given by the sum of the corresponding contributions in Figs. 10 and 11.

(solid lines) according to Eqs. (A10) and (7.7). The curves are separately plotted for the processes in Figs. 9(a) and 9(c), 9(d). The global antenna pattern from $\gamma\gamma$ collisions is essentially given by the sum of these contributions, as stated before. The angular dependence is very sharp in both cases. Then, the confinement corrections are positive and can be rather large, even if the corresponding broadening is relatively small, of $O(\langle p_T \rangle / M_H)$. In any case, the next correction is $O(\langle p_T \rangle / M_H)$ with respect to the first one. Therefore, Eqs. (A10) and (7.7), as well as the results in Figs. 10 and 17, should be a reliable approximation for confinement effects, even if the corrections are large.

The contribution from the process $\gamma\gamma \rightarrow \bar{q}q$ is roughly one order of magnitude larger than the $q\gamma \rightarrow qG$ contribution, in the regions which are shown in the figures. However, it is possible to get information on the photon structure functions if one requires events with a third jet which comes out very close to the beam direction.

The peculiarities of the antenna pattern from $\gamma\gamma$

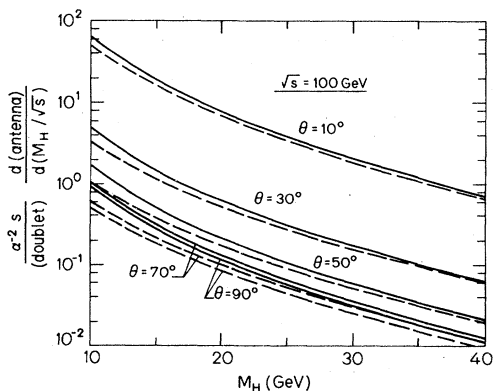


FIG. 12. Same as Fig. 10, but at $\sqrt{s} = 100$ GeV.

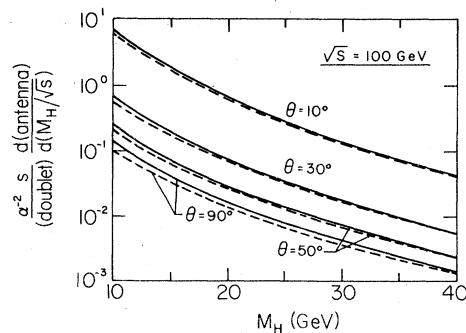


FIG. 13. Same as Fig. 11, but at $\sqrt{s} = 100$ GeV.

collisions (sharp angular distribution, strong dependence on M_H/\sqrt{s}) are important enough to encourage calorimetric experiments in this direction. As a second step, one could think of more accurate measurements of the antenna pattern such as to allow for a study of QCD scaling violations.

IX. SUMMARY AND CONCLUSIONS

In the first part of this work we have studied the background from $\gamma\gamma$ processes in calorimetric experiments. In order to measure the energy pattern for e^+e^- annihilation into hadrons to order $O(\alpha_s \alpha^2)$, one has to suppress this background by selecting events which have either hadronic energy or hadronic invariant mass larger than 60% or 70% of \sqrt{s} in the range of energies of PETRA or LEP. The two-photon contamination is less important in the energy correlation so that it can be eliminated by slightly weaker requirements. The de-

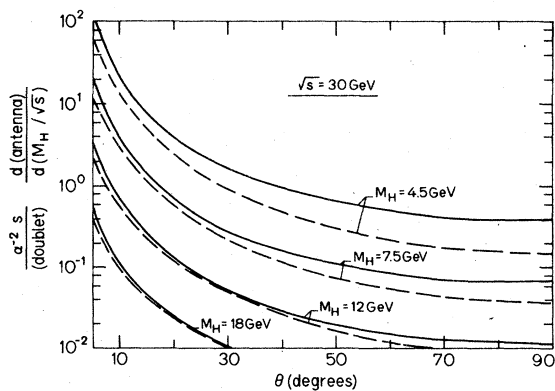


FIG. 14. Angular dependence of the antenna pattern for the process in Fig. 9(a), for several values of the hadronic mass, M_H , at $\sqrt{s} = 30$ GeV. Solid lines (dashed lines) are the results including (without) the confinement corrections.

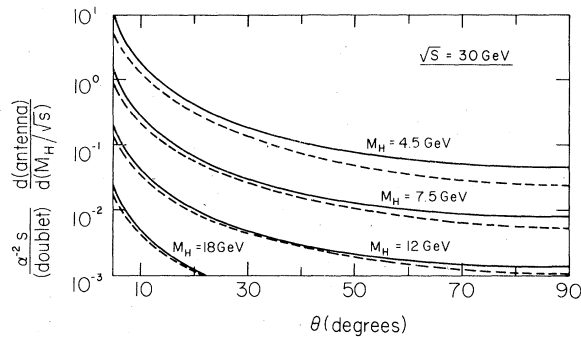


FIG. 15. Same as Fig. 14, but for the process in Fig. 9(c).

tailed results, which are discussed in Sec. IV, allow for an estimate of the different contributions to the antenna pattern and asymmetries in the energy correlation, with many possible experimental arrangements.

The corrections to the perturbative calculations from the nonperturbative effects of color confinement have been reliably evaluated and shown to be small as expected from the fact that the quark recombination is a soft process. We have also insisted on the necessity of measuring the s dependence of the energy pattern in order to eliminate (and study) the effects of the heavy-quark masses and weak decays.

Since (high-energy) $\gamma\gamma$ collisions should occur at large rates for \sqrt{s} in the range of PETRA or LEP, we encourage experimentalists to study the energy pattern in two-photon processes and we provide detailed predictions. In particular, we have discussed the antenna pattern for three-jet events which can afford interesting information on the photon structure functions. Unfortunately, the contribution from the (C -even) heavy-quark bound states are relatively small, and, in order to disentangle this contribution from the continuum background, the calorimeter should have an energy

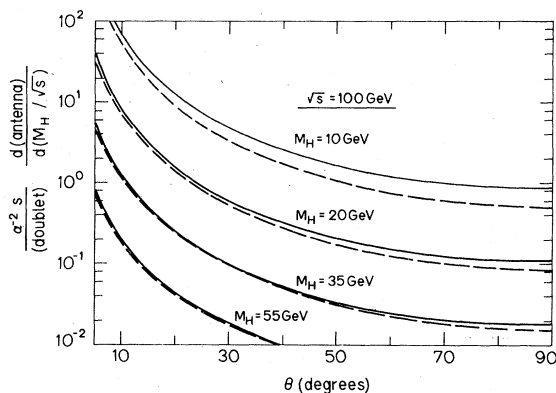


FIG. 16. Same as Fig. 14, but at $\sqrt{s} = 100$ GeV.

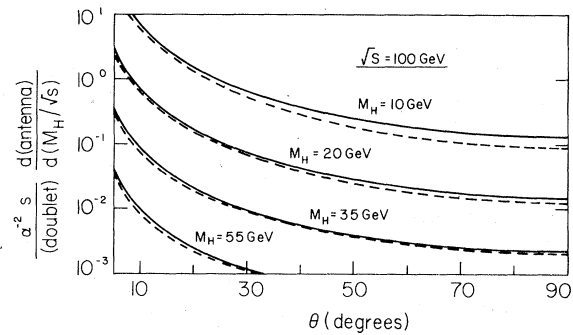


FIG. 17. Same as Fig. 15, but at $\sqrt{s} = 100$ GeV.

resolution which seems difficult to achieve.

An experimental study of the energy correlation in two-photon processes looks particularly attractive. The very typical angular dependence which is expected for this energy correlation has been stressed in Sec. IV. The interesting contribution from Eq. (7.8) (related to the QCD structure of the photon) has essentially the same behavior, but it is characterized by the presence of an additional jet along the beams.

Electron tagging would measure the corresponding (virtual) photon energy and mass. Our results are easily extended to this kind of experiment, insofar as the photon is almost on shell, so that the EPA can be applied by omitting the integrations in the variable v (the $\gamma\gamma$ c.m. velocity). A detailed study of the energy flow and resonance formation in two-photon physics with tagged electrons will be presented in a forthcoming paper.¹⁸

In conclusion, calorimetric experiments on photon-photon collisions should supply original information on the interplay between the strong and electromagnetic interactions at high energies. They would test both the perturbative (radiative corrections) and nonperturbative predictions (photon structure functions) of quantum chromodynamics.

ACKNOWLEDGMENTS

We are indebted to Dr. J. Field and to Professor J. C. Sens, for discussions. This research was supported in part by the Swiss National Science Foundation.

APPENDIX A

We argue in this appendix that the corrections from quark confinement to the antenna pattern of the process $\gamma\gamma \rightarrow \text{hadrons}$ should decrease as $\langle p_T \rangle / \sqrt{s}$. Let us introduce the fragmentation function $D(z, p_T)$ for (light) quarks into (light) hadrons, where $z = 2p_{||} / \sqrt{\hat{s}}$, p_T and $p_{||}$ are the transverse and longitudinal momenta of the hadron relative to the quark direction, and $\sqrt{\hat{s}}$ is the total energy of the two photons (everything being defined in the

2 γ c.m. system). Energy conservation fixes the normalization of the fragmentation function as follows (a summation over all final hadrons is understood hereunder):

$$\int_0^1 dz \int_0^\infty d^2\vec{p}_T z D(z, p_T) = 1. \quad (\text{A1})$$

The integration of $zD(z, p_T)$ over the phase space of the hadrons gives the mean multiplicity of the jet

$$\int dz \int d^2\vec{p}_T \frac{zD(z, p_T)}{(z^2 + 4p_T^2/s)^{1/2}} = \frac{\langle n \rangle}{2} = \frac{1}{2}(C \ln\sqrt{s} + \text{const}) \quad (\text{A2})$$

($\langle n \rangle$ being the mean multiplicity for two jets together), where C is a constant

$$\frac{C}{2} = \int d^2\vec{p}_T [zD(z, p_T)]_{z \rightarrow 0} \quad (\text{A3})$$

which is empirically ~ 2.5 . The average transverse momentum of the jet is

$$\begin{aligned} \langle p_T \rangle &= \frac{\int \frac{d^3\vec{p}}{2E} p_T z D(z, p_T)}{\int \frac{d^3\vec{p}}{2E} z D(z, p_T)} \\ &\approx \frac{2}{C} \int \frac{d^3\vec{p}}{2E} p_T [zD(z, p_T)]_{z \rightarrow 0}. \end{aligned} \quad (\text{A4})$$

The antenna pattern for $\gamma\gamma \rightarrow$ hadrons taking into account the fragmentation of the quarks is now

$$\begin{aligned} \frac{d\tilde{\Sigma}^*}{d\Omega^*} &= 2 \int \frac{d^3\vec{p}_i}{E_i} d\Omega_q \frac{d\sigma}{d\Omega_q}(\theta_q) z D(z, p_T) \frac{E_i}{\sqrt{s}} \\ &\quad \times \delta(\Omega_i - \Omega^*) \\ &= 2 \int p_i^2 dp_i \frac{1}{\sqrt{s}} d\Omega_q \frac{d\sigma}{d\Omega_q}(\theta_q) z D(z, p_T), \end{aligned} \quad (\text{A5})$$

$$\cos\theta_q = \cos\theta^* \cos\eta - \sin\theta^* \sin\eta \cos\phi,$$

where $\Omega_q = (\theta_q, \phi_q)$ are the angles defining the direction of the quark momentum and (η, ϕ) are the angles between the quark and the hadron. At high energies

$$\frac{d\sigma}{d\Omega_q}(\theta_q) = \frac{\alpha^2 Q^4}{s} \left(\frac{2}{\sin^2\theta_q} - 1 \right) \quad (\text{A6})$$

is the cross section for $\gamma\gamma \rightarrow q\bar{q}$. The factor of 2 in Eq. (A5) appears since the contribution from both jets are to be taken into account. Performing the integration over the azimuthal angle in (A5) with (A6)

$$\begin{aligned} \frac{d\tilde{\Sigma}^*}{d\Omega^*} &\equiv \frac{d\Sigma^*}{d\Omega^*} + \frac{d\Sigma_{cc}^*}{d\Omega^*} \\ &= \frac{2\alpha^2 Q^4}{\tau s} \int \frac{d^3\vec{p}}{\sqrt{\tau s}} z D(z, p_T) \left(\frac{2 \cos\eta}{\sin^2\theta^* - \sin^2\eta} - 1 \right), \end{aligned} \quad (\text{A7})$$

where $d\Sigma^*/d\Omega$ is the antenna pattern obtained [cf. Eq. (2.13)] by neglecting the corrections from the quark confinement [confinement corrections (cc)]. The latter is given by

$$\begin{aligned} \frac{d\Sigma_{cc}^*}{d\Omega^*} &= \frac{d\tilde{\Sigma}^*}{d\Omega^*} - \frac{d\Sigma^*}{d\Omega^*} \\ &= \frac{2\alpha^2 Q^4}{\tau s} \int dz d^2\vec{p}_T z D(z, p_T) \\ &\quad \times \left[\frac{\sin^2\eta - (1 - \cos\eta)\sin^2\theta^*}{\sin^2\theta^*(\sin^2\theta^* - \sin^2\eta)} \right], \end{aligned} \quad (\text{A8})$$

where

$$\begin{aligned} \cos\eta &= \frac{z}{(z^2 + 4p_T^2/s)^{1/2}}, \\ \sin\eta &= \frac{2p_T/\sqrt{s}}{(z^2 + 4p_T^2/s)^{1/2}}. \end{aligned}$$

The important contributions to the z integral in (A8) come from the region $z < p_T/\sqrt{s} \ll 1$. Assuming that $zD(z, p_T)$ is relatively smooth in this region, it can be replaced by its $z \rightarrow 0$ limit, and one gets from (A4),

$$\begin{aligned} \frac{d\Sigma_{cc}^*}{d\Omega^*} &= \frac{\alpha^2 Q^4}{\tau s} \int d^2\vec{p}_T [zD(z, p_T)]_{z \rightarrow 0} \left(\frac{2p_T}{\sqrt{s}} \right) I(\theta^*) \\ &= \frac{\alpha^2 Q^4}{s} \frac{C\langle p_T \rangle}{\sqrt{\tau s}} I(\theta^*), \end{aligned} \quad (\text{A9})$$

$$I(\theta^*) = \frac{1}{\sin^3\theta^*} \left[\tanh^{-1}(\sin\theta^*) + \frac{\pi}{2} - \sin\theta^* \right].$$

Using (A9) in (2.9b) after replacing θ^* with the expression in Eq. (2.4), one gets for the confinement correction to (2.9b)

$$\begin{aligned} \frac{d\Sigma_{cc}}{d\Omega} &= \frac{\alpha^2}{s} A_{\gamma\gamma}^{cc}(\theta, s), \\ A_{\gamma\gamma}^{cc}(\theta, s) &= \left(12 \sum_f Q_f^4 \right) C(s) \frac{C\langle p_T \rangle}{\sqrt{s}} \frac{1}{\sin^2\theta} \\ &\quad \times \int_{\tau_0}^1 \frac{d\xi}{\xi^3} \int_0^{(1-\xi)/\xi} dv \frac{H(\xi, v)}{(1-v^2)^{1/2}} F_{cc}(v, \theta), \end{aligned} \quad (\text{A10})$$

$$\begin{aligned} F_{cc}(v, \theta) &= \frac{1}{(1-v^2)^{3/2}} \left[\frac{\pi}{2} - \frac{(1-v^2)^{1/2} \sin\theta}{(1-v^2 \cos^2\theta)} \right. \\ &\quad \left. + \frac{1}{2} \ln \left| \frac{(1-v^2)^{1/2} + \sin\theta}{(1-v^2)^{1/2} - \sin\theta} \right| \right], \end{aligned}$$

with $H(\xi, v)$ as given in Eq. (2.15).

The importance of this correction is illustrated in Fig. 1. It is always positive and roughly proportional to $(\sin\theta)^{-3}$.

In an analogous way, one gets the corrections to the antenna pattern in the case (a) discussed in Sec. II. The corrected antenna pattern is obtained by adding to $A'_{\gamma\gamma}(\tau_0, \theta)$, defined in Eq. (2.18) the following term:

$$A'_{cc}(\tau_0, \theta) = 2 \left(3 \sum_f Q_f^4 \right) C(s) \frac{C\langle p_T \rangle}{\sqrt{s}} \frac{1}{\sin^3 \theta} \int_{\tau_0}^1 \frac{d\tau}{\tau^2} \int_0^{(1-\tau)/(1+\tau)} dv (1-v^2)^{1/2} \tilde{H}(\tau, v) F_{cc}(v, \theta), \quad (\text{A11})$$

where $\tilde{H}(\tau, v)$ and $F_{cc}(v, \theta)$ are respectively given by Eqs. (2.18) and (A10). This correction is shown in Fig. 2.

The analogous correction for $a(\tau, \theta)$ defined in Eq. (2.20) is obtained by suppressing the τ integration. Its effect is shown in Figs. 10 and 12. Notice that the correction can be quite large for small τ and large angles. However, the corrected result is still a good approximation, since the next correction is of order $O(p_T/\sqrt{\tau s})$ with respect to the first one.

APPENDIX B

We will calculate here the antenna pattern for the production of heavy quarks. The fragmentation of the quark into hadrons will be neglected for simplicity. The results will then be improved in Appendix C, where the confinement of quarks will be taken into account.

We assume that a pair of heavy quarks is produced with a differential cross section ($d\hat{\sigma}/d\Omega$) in the $\bar{Q}Q$ c.m. system. The heavy quarks will then weakly decay into light particles (π, K, μ, e, γ) which are observed (in general this process may occur through a cascade decay). The phase-space distribution of a final light particle i will be denoted ($2E_i d^3N_i/d^3\vec{p}_i$). The antenna pattern for such a process in the $\bar{Q}Q$ c.m. system is then,

$$\begin{aligned} \frac{d\Sigma^*}{d\Omega^*} &= 2 \sum_i \int \frac{d^3\vec{p}_i}{2E_i} \int d\Omega_q \frac{E_i}{(\hat{s})^{1/2}} \left(\frac{2E_i d^3N_i}{d^3\vec{p}_i} \right) \frac{d\hat{\sigma}}{d\Omega_q} \\ &\quad \times \delta(\Omega_i - \Omega^*) \\ &= \sum_i \int d\Omega_q \int \frac{E_i^2 dE_i}{(\hat{s})^{1/2}} \left(\frac{2E_i d^3N_i}{d^3\vec{p}_i} \right) \frac{d\hat{\sigma}}{d\Omega_q}. \end{aligned} \quad (\text{B1})$$

Introducing the energy of the particle i in the quark rest system

$$\begin{aligned} \epsilon_i &= \frac{E_i}{(1-\beta^2)^{1/2}} (1-\beta \cos \eta), \\ \beta &= \left(1 - \frac{4m_Q^2}{s} \right)^{1/2}, \end{aligned} \quad (\text{B2})$$

with β being the quark velocity and η the angle between the quark and the direction (θ^*, ϕ^*) of the particle i in the $\bar{Q}Q$ c.m. system, one gets

$$\begin{aligned} \frac{d\Sigma^*}{d\Omega^*} &= \int d\Omega_q \frac{d\hat{\sigma}}{d\Omega_q} \frac{(1-\beta^2)^2}{(1-\beta \cos \eta)^3} \\ &\quad \times \int \frac{\epsilon_i^2 d\epsilon_i}{2m_Q} \left(\frac{dN}{2\pi \epsilon_i d\epsilon_i} \right) \\ &= \frac{1}{4\pi} (1-\beta^2)^2 \int d\Omega_q \frac{d\hat{\sigma}}{d\Omega_q} \frac{1}{(1-\beta \cos \eta)^3} \end{aligned} \quad (\text{B3})$$

since, by energy conservation,

$$\int d\epsilon_i \epsilon_i \left(\frac{dN}{d\epsilon_i} \right) = m_Q. \quad (\text{B4})$$

With the partial-wave decomposition

$$\frac{d\hat{\sigma}}{d\Omega_q} = \sum_n \hat{\sigma}_n(\beta) P_n(\cos \theta_q), \quad (\text{B5})$$

$$\cos \theta_q = \cos \theta^* \cos \eta + \sin \theta^* \sin \eta \cos \phi,$$

one can perform the angular integration in (B3) to obtain

$$\frac{d\Sigma^*}{d\Omega^*} = \sum_n \hat{\sigma}_n(\beta) P_n(\cos \theta^*) R_n(\beta), \quad (\text{B6})$$

$$R_n(\beta) = \frac{1-\beta^2}{2\beta} Q_n^2\left(\frac{1}{\beta}\right), \quad R_0(\beta) = 1,$$

where $Q_n^2(x)$ is a Legendre function of the second kind. The weights $R_n(\beta)$ have the property

$$R_n(\beta) \xrightarrow{\beta \rightarrow 1} 1, \quad (\text{B7})$$

so that, for $\beta \rightarrow 1$, one recovers the simple relation

$$\frac{d\Sigma^*}{d\Omega^*} \rightarrow \sum_n \hat{\sigma}_n(1) P_n(\cos \theta^*) = \frac{d\hat{\sigma}}{d\Omega^*} \Big|_{\beta=1}, \quad (\text{B8})$$

which is valid for light quarks (up to confinement corrections). Notice that the resulting antenna pattern is independent of the quark-decay distribution. It depends on the fragmentation function in a simple way which will be discussed in Appendix C.

APPENDIX C

A more realistic calculation of the antenna pattern from heavy-quark production should also take quark confinement into account. The fragmentation of the heavy quark must produce a heavy hadron, which carries the heavy-quark flavor, plus a certain number of light hadrons (π 's, K 's), which we will call "primary." The heavy hadron will then weakly decay into light hadrons and lep-

tons, that will be designated as "secondary." (Notice that, for convenience we also include in the "primary" class the particles produced through the decay of, strictly speaking, primary hadrons.)

Correspondingly, we will separate the fragmentation function of the heavy quark into a light-primary-hadron part plus a heavy-hadron one,

$$D(z, p_T) = D_L(z, p_T) + D_H(z, p_T), \quad (C1)$$

which are normalized as follows:

$$\int dz d^2 \vec{p}_T z D_L(z, p_T) = \lambda,$$

$$\int dz d^2 \vec{p}_T z D_H(z, p_T) = 1 - \lambda, \quad (C2)$$

$$\int dz d^2 \vec{p}_T D_H(z, p_T) = 1,$$

where λ is the average energy lost by the heavy quark in its fragmentation and materialized into "primary" hadrons. From simple arguments¹⁷ the parameter λ is expected to be small for heavy quarks (an educated guess would be 0.2–0.3 for the b quark and 0.1–0.2 for a t quark of mass

~ 10 – 15 GeV). For very small values of z , we expect $D(z, p_T)$ to be dominated by $D_L(z, p_T)$ with a plateau height, defined as in Eq. (A3), quite similar to the light-quark one ($C \sim 2.5$).

The contribution of the light "primary" hadrons to the antenna pattern in the $Q\bar{Q}$ c.m. system is then,

$$\frac{d\Sigma_L^*}{d\Omega^*} = 2 \int \frac{d^3 \vec{p}_i}{2E_i} d\Omega_q \frac{d\hat{\sigma}}{d\Omega_q} z D_L(z, p_T) \frac{E_i}{\sqrt{s}} \delta(\Omega_i - \Omega^*). \quad (C3)$$

This contribution is analogous to Eq. (A5) and one can proceed in the same lines as in Appendix A and Ref. 1 to show that

$$\frac{d\Sigma_L^*}{d\Omega^*} = \lambda \frac{d\hat{\sigma}}{d\Omega^*} + \frac{d\Sigma_{cc}^*}{d\Omega^*}. \quad (C4)$$

The corrections from confinement have the same pattern as for light quarks, being proportional to $\langle p_T \rangle / \sqrt{s}$.

The contribution of the decay products of the heavy hadron to the antenna pattern in the $Q\bar{Q}$ c.m. system is

$$\frac{d\Sigma_H^*}{d\Omega^*} = 2 \sum_i \int \frac{d^3 \vec{p}_i}{2E_i} \int \frac{d^3 \vec{p}_H}{2E_H} \int d\Omega_q \frac{d\sigma}{d\Omega_q} z D_H(z, p_T) \left(\frac{2E_i d^3 N_i}{d^3 \vec{p}_i} \right) \frac{E_i}{\sqrt{s}} \delta(\Omega_i - \Omega^*), \quad (C5)$$

where the indices H and i refer to the heavy hadron and to the final light particles, respectively; $\hat{\sigma}$ and N_i are defined as in Appendix B. Performing the trivial integrations and using Eq. (B4), one gets

$$\frac{d\Sigma_H^*}{d\Omega^*} = \int \frac{d\Omega_q}{4\pi} dz d^2 \vec{p}_T z D_H(z, p_T) \frac{d\hat{\sigma}}{d\Omega_q} \frac{(1 - \beta_H^2)}{(1 - \beta_H \cos\eta)^2}, \quad (C6)$$

$$\beta_H = \frac{(1 + \beta)z - (1 - \beta)}{(1 + \beta)z + (1 - \beta)},$$

where $\cos\eta$ is the angle between the hadron H and the calorimeter direction (θ^*, ϕ^*). As far as confinement is concerned, we expect the \vec{p}_T distribution of heavy hadrons to be roughly the same as that of the light "primary" hadrons. The angle between the heavy hadron and the heavy quark is then of the order of $2\langle p_T \rangle / \langle z \rangle \sqrt{s} = 2\langle p_T \rangle / (1 - \lambda)\sqrt{s}$. One can take into account this angle by applying to Eq. (C6) the same procedure as in Appendix A and Ref. 1. However, since $z D_H(z, p_T)$ is expected to be very small for $z \rightarrow 0$, this would just lead to negligible correction. Therefore, one can safely identify the angle η to that between the heavy quark and the calorimeter direction, and perform the

angular integration in (C6) on the same lines as in Appendix B to obtain

$$\frac{d\Sigma_H^*}{d\Omega^*} = \sum_n P_n(\cos\theta^*) \hat{\sigma}_n(\beta) \times \int dz d^2 \vec{p}_T z D_H(z, p_T) R_n(\beta_H), \quad (C7)$$

where the partial waves, $\sigma_n(\beta)$, and the weights, $R_n(\beta_H)$, are defined as in Appendix B. By using Eq. (C2), this result can also be written as

$$\frac{d\Sigma_H^*}{d\Omega^*} = (1 - \lambda) \frac{d\hat{\sigma}}{d\Omega^*} - \sum_n P_n(\cos\theta^*) \hat{\sigma}_n(\beta) \bar{S}_n(\beta), \quad (C8)$$

where

$$\bar{S}_n(\beta) = \int dz d^2 \vec{p}_T z D_H(z, p_T) [1 - R_n(\beta_H)], \quad (C9)$$

$$\bar{S}_0 = 0, \quad \bar{S}_n \xrightarrow{\beta \rightarrow 1} 0.$$

Finally, the total antenna pattern from heavy quark in the $Q\bar{Q}$ c.m. system is obtained by adding Eqs. (C4) and (C8)

$$\frac{d\Sigma^*}{d\Omega^*} = \frac{d\hat{\sigma}}{d\Omega^*} - \sum_n P_n(\cos\theta^*) \hat{\sigma}_n(\beta) \bar{S}_n(\beta) + \frac{d\Sigma_{cc}^*}{d\Omega^*}. \quad (C10)$$

APPENDIX D

It has been stressed in Sec. VI that the antenna pattern for heavy-quark production may be very different from the light-quark one. Both the rather persistent threshold effects and the heavy-hadron decay will affect the ultrarelativistic limit which is usually assumed in light-quark calculations. Remarkably enough, the effects of the quark masses are easily estimated. A very simple general formalism is presented in Appendix B, which is just an extension to the antenna pattern of the approach developed in Ref. 14.

These results will be applied here to the one-photon production of heavy quarks in e^+e^- collisions, i.e., $e^+e^- \rightarrow \gamma^* \rightarrow \bar{Q}Q$. The cross section for this process is

$$\frac{d\hat{\sigma}}{d\Omega} = \frac{3\alpha^2 Q^2}{4s} \beta(2 - \beta^2 + \beta^2 \cos^2\theta), \quad (D1)$$

$$\beta = \left(1 - \frac{4m_Q^2}{s}\right)^{1/2},$$

and the antenna pattern, once the heavy hadron decay is taken into account, is obtained from Eq. (B6) as follows:

$$\frac{d\Sigma_Q}{d\Omega} = \frac{d\hat{\sigma}}{d\Omega} - \frac{1}{2} \sigma_2(\beta)[1 - R_2(\beta)](3 \cos^2\theta - 1), \quad (D2)$$

where σ_2 is the $D_2(\cos\theta)$ component of Eq. (D1),

$$\sigma_2(\beta) = \frac{\alpha^2 Q^2}{2s} \beta^3, \quad (D3)$$

and the definition, Eq. (B6), of $R_2(\beta)$ gives

$$1 - R_2(\beta) = \frac{3(1 - \beta^2)}{2\beta^2} \left[1 - \frac{(1 - \beta^2)}{\beta} \tanh^{-1}\beta\right]. \quad (D4)$$

Putting everything together, one gets for the antenna pattern for $e^+e^- \rightarrow \bar{Q}Q$,

$$\begin{aligned} \frac{d\Sigma_Q}{d\Omega} &= \frac{\alpha^2}{s} A_Q(s, \theta), \\ A_Q(s, \theta) &= \frac{3Q^2}{4} \beta \left[\frac{3 - \beta^2}{2} (1 + \cos^2\theta) \right. \\ &\quad \left. - \rho(\beta)(3 \cos^2\theta - 1) \right], \quad (D5) \\ \rho(\beta) &= (1 - \beta^2) \left(1 - \frac{1 - \beta^2}{2\beta} \tanh^{-1}\beta\right). \end{aligned}$$

These results are valid in the limit where the energy loss in the fragmentation of the heavy quark into a heavy hadron is neglected. They can be corrected for this confinement effect, as shown in Appendix C, by replacing the weight, Eq. (D4), by its effective value:

$$\bar{S}_2(\beta) = \int dz d^2 \vec{p}_T z D_H(z, p_T) [1 - R_2(\beta_H)], \quad (D6)$$

$$\beta_H = \frac{(1 + \beta)z - (1 - \beta)}{(1 + \beta)z + (1 - \beta)}.$$

As already noticed in Sec. VI, these confinement effects should not be very important for heavy quarks.

¹C. L. Basham, L. S. Brown, S. D. Ellis, and S. T. Love, Phys. Rev. D **17**, 2298 (1978); Phys. Rev. Lett. **41**, 1585 (1978).

²G. Tiktopoulos, Nucl. Phys. **B147**, 371 (1979).

³See, e.g., the recent work of R. Field and R. P. Feynman, Nucl. Phys. **B136**, 1 (1978), and references therein.

⁴See, e.g., S. J. Brodsky, in *Proceedings of the 1971 International Symposium on Electron and Photon Interactions at High Energies*, edited by N. B. Mistry (Laboratory of Nuclear Studies, Cornell University, Ithaca, 1972), p. 20.

⁵There are several excellent reviews of $\gamma\gamma$ physics, including very complete bibliographies: H. Terazawa, Rev. Mod. Phys. **45**, 615 (1973); S. J. Brodsky, Ref. (4); N. Budnev *et al.*, Phys. Rep. **15C**, 181 (1975); LEP Study Group Yellow Report, CERN Report No. 76-18 (unpublished); PEP Summer Studies, 1974, 1975 (unpublished); Collège de France $\gamma\gamma$ Colloquium [J. Phys. (Paris) Suppl. **35** (1973)]; P. V. Landshoff, in *Proceedings of the LEP Summer Study CERN Yellow report No. 79-01, 1979* (unpublished), p. 555.

⁶For a discussion of the validity of the equivalent photon approximation, see, e.g., G. Bonneau, M. Gourdin, and F. Martin, Nucl. Phys. **B54**, 573 (1973); R. Bhat-

tacharya *et al.*, Phys. Rev. D **15**, 3267 (1977); **15**, 3280 (1977); V. N. Baier and V. S. Fadin, Zh. Eksp. Teor. Fiz. Pis'ma Red. **13**, 293 (1971) [JETP Lett. **13**, 208 (1971)]; Refs. 4 and 5.

⁷For recent quantitative evaluation of these experimental cuts, see, e.g., J. Field, in *Proceedings of the LEP Summer Study*, CERN Yellow Report No. 79-01, 1979 (unpublished), p. 563. M. Davier, in *Proceedings of the LEP Summer Study CERN Yellow Report No. 79-01, 1979* (unpublished), p. 61, and Ref. 5.

⁸R. Gatto and G. Preparata, Lett. Nuovo Cimento **7**, 507 (1973); M. Ahmed and G. Ross, Phys. Lett. **59B**, 293 (1975); K. J. Evans, P. V. Landshoff, and J. C. Polkinghorne, Phys. Rev. D **12**, 2082 (1975); M. Greco and Y. Srivastava, Nuovo Cimento **43A**, 88 (1978).

⁹E. Witten, Nucl. Phys. **B120**, 189 (1977); C. Llewellyn Smith, Phys. Lett. **79B**, 83 (1978); W. Frazer and J. F. Gunion, Phys. Rev. D **19**, 2447 (1979).

¹⁰S. J. Brodsky *et al.*, Phys. Rev. Lett. **41**, 672 (1978); Phys. Rev. D **19**, 1418 (1979); S. J. Brodsky, Phys. Scr. (to be published); K. Kajantie, Helsinki Report No. HU-TFT-79-5, 1979 (unpublished).

¹¹E. Eichten and K. Gottfried, Phys. Lett. **66B**, 286 (1977).

¹²M. Krammer and P. L. Ferreira, Rev. Bras. Fis. **6**, 7 (1976); C. Quigg and J. L. Rosner, Phys. Rev. D **17**,

- 2364 (1978); J. S. Bell and J. Pasupathy, *Phys. Lett.* 83B, 389 (1979).
- ¹³V. A. Novikov *et al.*, *Phys. Rep.* 41C, 1 (1978).
- ¹⁴R. Gatto and I. Vendramin, *Nuovo Cimento* 41A, 125 (1977). See also R. Gatto, in Proceedings LXXI Course at Fermi school, Varenna and report Université de Genève (unpublished).
- ¹⁵After the completion of this work, we received a report by W. A. Bardeen and A. J. Buras [*Phys. Rev. D* 20, 166 (1979)] where these corrections are computed.
- ¹⁶C. T. Hill and G. G. Ross, *Nucl. Phys.* B148, 373 (1979). See, however, Ref. 15.
- ¹⁷J. D. Bjorken, *Phys. Rev. D* 17, 171 (1978).
- ¹⁸G. Anastaze, R. Gatto, and C. A. Savoy (in preparation).